Bio-inks for 3D Bioprinting: Recent Advances and Future Prospects

Ilze Donderwinkel[a,b], Jan C.M. van Hest[b,c], Neil R. Cameron*[a,d]

[a] Department of Materials Science and Engineering, Monash University, Clayton, 3800 VIC, Australia

[b] Department of Bio-organic Chemistry, Radboud University, 6525 AJ Nijmegen, the Netherlands

[c] Department of Chemical Engineering and Chemistry, TU Eindhoven, 5600 MB Eindhoven, the Netherlands

[d] School of Engineering, University of Warwick, Coventry CV4 7AL, U.K.

ABSTRACT: In the last decade, interest in the field of three-dimensional (3D) bioprinting has increased enormously. 3D bioprinting combines the fields of developmental biology, stem cells, and computer and materials science to create complex bio-hybrid structures for various applications. It is able to precisely place different cell types, biomaterials and biomolecules together in a predefined position to generate printed composite architectures. In the field of tissue engineering, 3D bioprinting has allowed the study of tissues and organs on a new level. In clinical applications, new models have been generated to study disease pathogenesis. One of the most important components of 3D bio-printing is the bio-ink, which is a mixture of cells, biomaterials and bioactive molecules that creates the printed article. This review describes all the currently used bio-printing inks, including polymeric hydrogels, polymer bead microcarriers, cell aggregates and extracellular matrix proteins. Amongst the polymeric components in bio-inks are: natural polymers including gelatin, hyaluronic acid, silk proteins and elastin; and synthetic polymers including amphiphilic block copolymers, PEG, poly(PNIPAAM) and polyphosphazenes. Furthermore, photocrosslinkable and thermoresponsive materials are described. To provide readers with an understanding of the context, the review also contains an overview of current bio-printing techniques and finishes with a summary of bio-printing applications.

INTRODUCTION

Additive manufacturing (AM), more commonly known as 3D printing, is a rapidly growing field of interest that fabricates physical objects by depositing material layer-by-layer according to a digital model. In the biomedical field, 3D bioprinting refers to several different AM techniques, which are able to print not only materials but also living cells, in a specified location. 3D bioprinting was first demonstrated in 1988 by Klebe,[1] who used the term 'cytoscribing' to describe the technique of the precise positioning of cells on a 2D substrate using a computer-controlled ink jet printer or graphics plotter. As more research groups joined, the technique evolved and the first international workshop on bioprinting and biopatterning was held in 2004 at the University of Manchester.[2] Between 2012 and 2015, the number of papers referring to bioprinting increased fourfold and new journals were introduced.[3] Currently, the field is expanding at a rapid rate.

The reason for the increasing popularity of 3D bioprinting is its tremendous potential. The aim of 3D bioprinting is to construct, *in vitro*, tissues, organs and other biological systems that mimic their native counterparts.[4] The materials used consist of natural and synthetic polymers, living cells, drugs, growth factors and genes. When deposited in a precise and controlled way, these allow the fabrication of not only scaffolds and scaffold-free tissues, but also mini-tissues and organ-on-a-chip models through different techniques.[5, 6] Depending on the type of tissue and aim of the fabrication, different bioprinting techniques can be used, including droplet-based, extrusion-based, laser-induced forward transfer, and integrated bioprinting. Each printing technique is based on different physical processes which define the criteria (i.e. rheology profile, photoreactivity, thermal and oxidative stability) of a suitable bioink. Due to its ability to precisely print cells whilst maintaining cell viability, 3D printed

tissues can be used in tissue engineering and regenerative medicine, transplantation, drug testing and high-throughput screening, and cancer research.

In tissue engineering and regenerative medicine, 3D bioprinting allows the development of 3D tissue models that can replace current 2D cell culture and animal models for *in vitro* drug testing. Animals respond differently to drug candidates compared to humans and therefore can be ineffective as models of human diseases.[5] 3D bioprinting can, furthermore, be used to print bone and cartilage for musculoskeletal injury repair. In in-situ bioprinting, the bio-ink is directly printed into the lesion sites during surgery, which places additional scrutiny on aspects of sterility and biocompatibility.

Due to a scarcity of patient-compatible donor tissue and organs, there is an increasing demand for tissue engineering solutions, including 3D bioprinted tissues. Through 3D printing, personalized tissues can be fabricated using anatomical 3D image analysis and computed tomography techniques.[4, 7] However, the technique is still at its early stage and many challenges have to be faced for transplantation and other applications.

Human tissues consist of many different cell types and are vascularized to allow transport of nutrients, oxygen and waste products. For successful tissue replacement in human patients, a vascular system has to be built-in at a single-cell level and heterocellular tissue patterning should be anatomically accurate.[5, 8-10] Furthermore, the materials used should be biocompatible, biodegradable, and should not have any toxic effect, including their waste compounds and intermediates. Bio-inks that are consistent with these requirements should also be bioprintable and enable rapid cell growth and proliferation.[5] Besides the materials used to create the neo-tissue, the printing technique itself (resolution, speed, and bioprinting processes) must also be optimized to allow fabrication of complex tissues at various scales.[4] 3D bioprinting has several advantages in this context. There is precise

control over size, microarchitecture and cellular composition.[11] It has a high-throughput capability in tissue model fabrication. Cells can be co-cultured with a low risk of cross-contamination.[12] Printed tissues should recreate the complexity and heterocellularity of native tissues. 3D bioprinting enables vascularization within the printed tissue, although this has to be explored further.

3D bioprinting is an interdisciplinary field, requiring knowledge from developmental biology, stem cell science, chemistry, computer science, and materials science.[13] To fabricate complex tissues that can be used for tissue replacement or for drug testing models, several conditions must be kept in mind.[6] There is a wide selection of materials that can be used for the bio-ink and scaffold; depending on the type of tissue, different cell types are needed. Stem cells have to differentiate into the cell type of interest, for which growth and differentiation factors are needed. In order to fabricate a 3D bioprinted tissue, cells have to survive the printing process, for which the sensitivity and protection of the cells is important. Cell viability after bio-printing can be identical to that obtained using the same bio-ink in a manual scaffolding process, depending on the type of bio-ink and printing process used[14]. The bioprinter itself thus plays an important role in the fabrication process. As tissues and organs are highly complex, a bioprinter should be able to print these different cell types and accompanying biomaterials at the same time.[11] The printed structure should be of a high resolution, which is also dependent on the accuracy of the printer. Other requirements of a bioprinter include: sufficient build speed, user friendliness, full automation capability, ease of sterilization, affordability, versatility, and compactness.[15]

This review focuses on the materials used in 3D bio-printing: the 'bio-inks'. Current advances and limitations will be discussed as well as future perspectives. It is complementary to the excellent recent review on bio-inks by Ozbolat et al., which provides a practical comparison between different

types of bio-inks.[16] In our review, we have included sections describing current bioprinting techniques and applications of 3D bioprinting, to enable the reader to understand better the context.

BIOPRINTING TECHNOLOGY

For the fabrication of 3D bioprinted constructs, the bio-ink and bioprinter are key elements. Important factors such as strength, resolution and shape are dependent on the fabrication method. Below, an overview of the most important bioprinting technologies are discussed. The main technologies are droplet-based, extrusion-based, laser-induced forward transfer, stereolithography, and integrated bioprinting (Figure 1). For a more thorough explanation of any of these technologies, the reader is directed to the recent review of Jungst *et al.*[17]

Droplet-based bioprinting

Droplet-based bioprinting (DBB), first introduced in the early 2000s,[11] is a simple and agile technique with which biologics can be deposited in a precise and controlled way. Picolitre droplets are layered on top of a substrate without contact between the nozzle and the substrate.[18] DBB is highly versatile as it is compatible with many biological materials, it can print inks with low viscosities (3.5-12 $mPa.s^{-1}$), and it enables a high speed and high resolution.[5, 11] However, it faces some challenges. The uniformity of the droplets needs to be improved and encapsulation of cells is inconsistent.[11] Furthermore, bioprinted constructs have a limited mechanical and structural integrity.[5] Cross-contamination of bio-inks when printed simultaneously restricts the size of the constructs as vascularization and porosity are hard to control.[5, 11] DBB can be subdivided into three categories; inkjet, acoustic, and micro-valve bioprinting (Figure 2).

Inkjet bioprinting

Inkjet bioprinting is the most common form of DBB.[11] It includes continuous-inkjet, drop-on-demand inkjet, and electrodynamic inkjet bioprinting. In continuous-inkjet bioprinting, the bio-ink solution in the chamber is extruded through a nozzle causing the stream to break up into droplets, due to the Rayleigh-Plateau instability (Figure 2A1).[5] The drop-on-demand (DOD) inkjet technique generates droplets using thermal or piezoelectric actuators, or electrostatic forces. This technique is preferred over continuous-inkjet bioprinting as it only generates droplets when required.[5] Droplets are generated by the breaking of surface tension rather than an applied pressure. Advantages of this technique are its low cost, high resolution (20-100μm) and deposition of multiple types of materials by using multiple nozzles.[18] The technique however has disadvantages. There is a narrow material selectivity as the technique only works for low viscosity liquids. The small size of the droplets increases the processing time and the printed tissue has weak mechanical properties.[18]

One way of generating droplets in DOD is through heating. When a voltage pulse is applied, the bio-ink solution is locally heated, producing a vapour bubble that then expands rapidly and bursts. The pressure produced by this pulse will at some point overcome the surface tension at the nozzle orifice, causing droplet ejection (Figure 2A2).[5] A great advance of this technique is that the integrity of stem cells is maintained; studies showed no loss in functionality and differentiation capacity, or a change in genotype and phenotype.[19, 20]

In piezoelectric-induced droplet formation, a piezoelectric actuator causes deformation in the fluid chamber after a pulse is applied[5]. The sudden change causes a pressure wave, which overcomes the surface tension at the nozzle orifice and causes droplet ejection (Figure 2A3). This technique

results in high resolution patterns, but a decreased cell viability compared to other techniques.[18] An electrostatic printed droplet is generated by a temporal increase in volume of the fluid chamber, caused by applying a voltage pulse between an electrode and a pressure plate. The pressure plate deflects, and restores to its original position when the pulse extinguishes. The increase in volume caused by the pressure plate causes ejection of the droplets (Figure 2A4).[5]

The third subset of inkjet bioprinting is electrohydrodynamic jet bioprinting, which uses an electric field to pull the droplet through the nozzle orifice. An advantage of this approach is the ability to use small nozzle orifice diameters and highly concentrated bio-inks.[5] However, due to the large shear forces produced from the high pressure on the droplets and the minuscule orifice diameter, cells can be damaged.[5] In the resting phase, the bio-ink is pushed to the orifice by a certain back-pressure so the bio-ink will form a spherical meniscus at the tip due to surface tension. A high voltage (0.5-20kV) is applied between the nozzle and the substrate, creating an electric field that causes the mobile ions in the bio-ink to accumulate near the surface of the meniscus. Due to Coulombic or electrostatic repulsions between these ions, the meniscus is deformed into a conical shape, the Taylor cone.[5] When the electrostatic stresses overcome the surface tension the droplet is ejected (Figure 2A5). Different jetting modes can be used with this technique and are dependent on the applied voltage, bio-ink properties, and bio-ink flow rate. These factors also determine the cell viability. At low voltages and flow rates, the printer is in dripping mode. For a more distinct stream of droplets, intermediate voltages and/or flow rates can be applied. For a continuous stream of bio-ink, a high voltage must be applied. The latter mode, also known as the cone-jet-mode, has a continuous presence of the Taylor cone.[5] The droplet size increases with the applied voltage. Droplet size is important in electrohydrodynamic jet bioprinting, as the media transport will be ineffective when it

exceeds 400 μm. Media transport is also affected by the bio-ink constituents, which affect the diffusion of the media, together with the cell concentration. Cell concentration, bio-ink constituents and the applied voltage together affect the long-term fate of the post-bioprinting cell. In general, the stream of droplets and continuous modes are used more often than the dripping mode. This makes this bioprinter less suitable for printing tissues that require accurate placement of the cells.[5]

Acoustic-droplet-ejection bioprinting

In acoustic-droplet-ejection bioprinters, the bio-ink is not exposed to stressors like heat, high pressure, high voltage or shear stress as in inkjet bioprinting. Rather, the bio-ink is kept in an open pool and droplets are produced through acoustic waves. The bio-ink in the reservoir is held in place due to the surface tension at a small exit channel. The bioprinter contains a single channel or an array of these 2D microfluidic channels. The acoustic actuator consists of a piezoelectric substrate with interdigitated gold rings placed upon it, which generate acoustic waves on demand on the surface (Figure 2B).[5] The generated circular waves move from the air-bio-ink interface down toward the exit channel to form an acoustic focal point. When the force of this focal point exerts the surface tension at the exit channel, a droplet will be ejected.[5] As the acoustic waves are critical for droplet ejection, any disturbances by a moving print head and/or substrate can interfere with the printing process by losing control over droplet ejection. Another disadvantage of the acoustic bioprinting technique is the inability to print with viscous bio-inks containing a high cellular concentration, such as commonly used hydrogels.[5]

Micro-valve bioprinting

In a micro-valve bioprinter, droplets are generated by the opening and closing of a microvalve under pneumatic pressure.[18] The printer contains a solenoid coil and a plunger that blocks the orifice. When a voltage pulse is applied, the valve coil at the top of the print head will generate a magnetic field which pulls the plunger upwards, unblocking the exit. When the back pressure in the bio-ink chamber is large enough and exceeds the surface tension, the bio-ink is ejected (Figure 2C).[5] This can either be in a continuous or dripping mode, depending on the back pressure and valve-gating time.

The droplet volume and cell viability are dependent on the pneumatic pressure of the microvalve, the nozzle geometry, the cell concentration, and the bio-ink constituents.[5] The volume of micro-valve bioprinter droplets are generally larger when identical nozzles are used, in comparison with other DBB techniques,[5] which reduces resolution. The cells printed through micro-valve bioprinting retain their function, are able to proliferate, and their genotype and phenotype are preserved.[21] Studies have shown that the differentiation capacity of stem cells is unaffected by the printing process.[22, 23] These characteristics make micro-valve bioprinting favorable for printing various types of cells and proteins.

Extrusion-based bioprinting

Extrusion-based printing was introduced in the early 2000s and is the most common and affordable bioprinting technique.[11] It is able to fabricate 2D and 3D structures by continuous dispersion of a hydrogel containing cells through a micro-nozzle.[18] Extrusion-based printers disperse the bio-ink through a pneumatic or mechanical system.[24] The 2D patterns are created by physically or chemically solidifying the hydrogels. By stacking these 2D patterns, 3D structures can be created.[18] The

advantages of this technique are the ability to deliver multiple cells and materials, and there is a wide material selectivity. It has the ability to disperse high viscous bio-inks with high cell densities, cell pellets,[25] tissue spheroids,[26, 27] and tissue strands.[28] Furthermore, the production is scalable and synthetic polymers can be used. A great advantage is the high cell viability, typically above 90%.[18] The technique however has a downside, as it has a relatively low resolution (>100µm). Ozbolat *et al*. created an extrusion-based 'Multi-arm Bioprinter' that is capable of multi-material deposition, has a reduced fabrication time, while being able to process multiple cell types at the same time[29]. This enables the printer to fabricate complex structures that can be organized like native tissue. Several tissue types have already been explored for extrusion-based bioprinting, including cartilage[30, 31], heart valve conduits[32, 33], and neuronal tissue[25, 34].

Very recently, Liu *et al.* created a rapid continuous multimaterial extrusion bioprinter that is able to print up to 7 different types of bio-inks without the need to switch nozzles.[35] The printer consists of different channels, each connected to its own bio-ink reservoir. Software is used to open the valves to deposit the different inks at the desired moment through a digitally tunable pneumatic single-printhead system. The advantage of this approach is the almost complete absence of a gap between the switching processes.[35] In order to test their printer, Liu *et al.* printed a range of complex 3D structures from multilayer cubes composed of 2 or 3 different bio-inks to human organ-like constructs from multiple bio-inks (Figure 3).

Laser-induced forward transfer bioprinting

Laser-induced forward transfer (LIFT) bioprinting was first introduced in 1999[36] for the deposition of inorganic materials and was soon after adapted for bioprinting.[37] The system contains a donor layer

with a ribbon structure, containing an energy-absorbing layer (gold or titanium), which responds to laser stimulation.[38] A layer of bio-ink is suspended on the bottom of the donor layer. During printing, a laser pulse is applied on the donor layer, heating a small portion. This creates a high-pressure bubble as part of the donor layer will evaporate. The high-pressure bubble puts pressure on the bio-ink layer, which propels the bio-ink towards the substrate underneath it. The bio-ink falling on the substrate will then immediately be crosslinked.[38] This non-contact printing method has a few advantages. First of all there is no contact between the dispenser and the bio-inks, taking away a contamination source. Furthermore, highly viscous materials can be used and the cell viability is high (>95%).[38] However, the laser can potentially damage the cells and the technique has a high associated cost. For these reasons only a few groups have investigated the capabilities of laser-induced forward transfer bio-printing. A LIFT study by Koch *et al*.[39] showed a survival rate of 98% for skin cells (fibroblasts, keratinocytes) and over 90% for human mesenchymal stem cells (hMSCs). Furthermore, all maintained their ability to proliferate and did not show any increase in apoptosis or DNA fragmentation.

Stereolithography

Another interesting bio-printing method is stereolithography which uses light to selectively crosslink bio-inks in a layer-by-layer process.[24] Instead of heating a donor layer as in laser-induced forward transfer printing, stereolithography uses a laser or digital light projector to photolytically crosslink the bio-inks, enabling it to crosslink a layer in a single printing plane.[38] The print head, therefore, only has to move in one direction. Advantages of stereolithography are its high resolution (<100µm), short printing time (<1h), and high cell viabilities (>90%).[38]

Integrated bioprinting

A general disadvantage of all bioprinting techniques is the low strength of the printed structures. Different research groups therefore have created hybrid techniques to improve the mechanical properties of the resulting constructs. For instance, Kang *et al*. created a hybrid system able to print with a synthetic biopolymer and a cell-laden hydrogel to fabricate a tissue construct with high mechanical strength.[18] In 2014, Pati *et al.* introduced a hybrid technique that could print relatively stiff biodegradable thermoplastic polymers and hydrogels containing decellularized extracellular matrix (dECM).[40] To be able to print human-scale functional tissue constructs, Kang *et al.* developed the integrated tissue-organ printer (ITOP). This printer was able to fabricate mandible and calvarial bone, cartilage and skeletal muscle.[41]

Design and printing strategies

The process capabilities of a bioprinter and design strategies are very important for 3D bioprinting.[42] Important design factors include shape and resolution, material heterogeneity, and cellular-material remodeling dynamism. Specific process capabilities, parameters and features should be mapped into these design factors. For successful bioprinting, design, technology and material selection should be considered carefully as these factors affect the integrity of the bioprinted structure. An in-depth discussion of these factors is beyond the scope of this review, for further information the reader is directed to the recent review by Lee *et al.*[42]

BIO-INKS

Bio-inks are biomaterial solutions containing the living cells and so are key components in bioprinting. It is important that the materials present in the biomaterial solution protect the cells against stressors during the printing process. The four main types of bio-ink materials are hydrogels, microcarriers, cell aggregates, and decellularized matrix components.[11, 43] Cell aggregates can be further classified into three subsets: tissue spheroids; cell pellets; and tissue strands.[11]

In DBB, besides protecting the cells against stressors, bio-ink droplets should also result in precise deposition. An important characteristic for this is droplet integrity, which can be altered by the material components of the bio-ink.[5] If this integrity is lost, the droplet can splash or spread, either displacing the deposited cells from their desired position or causing structural failure.[5] After collision with the substrate, a droplet can disintegrate into secondary droplets (splashing), or expand its surface area (spreading). The type of collision is dependent on the droplet size, density, and surface tension.[5]

In extrusion-based printing, bio-inks should have certain viscoelastic characteristics, including shear-thinning and self-healing properties.[24] Shear-thinning is important for the extrusion of the bio-ink at low nozzle pressures to protect the cells against physical stressors. The bio-ink should then be able to self-heal to keep an integer 3D printed structure.[24] For a structurally stable complex with mechanical integrity, the bio-ink should harden, in a cytocompatible manner, immediately after printing. In tissue regeneration, the scaffold structure should be degraded by the body to allow integration of the new tissues.[24]

In tissue engineering, constructs are needed with which to fabricate both hard and soft tissues. Many studies have already shown the potential in hard tissue engineering by the fabrication of tissues like cartilage and bone.[44-46] However, challenges still remain. For instance, patient-specific treatment

needs optimization and, more importantly, printing of large size and uniform constructs has not yet been achieved.[4] A specific challenge lies in soft tissue engineering. As soft tissues have a combination of highly elastic, flexible and viscous properties, stacking of layers is difficult.[6] For both hard and soft tissue engineering, different bio-inks can be used to create a structure with the right properties for a certain application. Several types of bio-inks will be discussed below (the properties and characteristics of the materials used in bio-inks are summarised in Table 1).

Hydrogels

A commonly used material for bio-inks are hydrogels, which are hydrated networks of crosslinked natural or synthetic polymers. The hydrophilic nature of these polymers allows the gel to swell in an environment with a high water content. Hydrogel materials can be both highly biocompatible and biodegradable, a necessity for *in vivo* applications. Furthermore, cells can be encapsulated in 3D when the hydrogel undergoes gelation.[6, 47, 48] The environment created does not affect cell-cell interactions.[49] A disadvantage of hydrogels, however, is their weak mechanical properties. They often do not maintain their designed shape.[50] Whether a hydrogel is suited or not for 3D bioprinting depends mainly on its rheological properties and the crosslinking method employed, which can be both physical and chemical in nature.[51] Several properties that influence printability and cell survival are summarized in Figure 4, these include gelation, viscosity, nozzle gauge, shear stress, network properties, and fabrication time.[51]

The residual structural and mechanical properties in the printed article are highly important for 3D bioprinting, as without these characteristics the function of the construct is lost. Several hydrogels have been explored employing a divergent set of synthetic and natural polymers, with and without

crosslinking to control properties.[6] The advantages of synthetic materials are that they can be tailored with specific physical properties, they have robust mechanical properties and good control over degradation time after the tissue is fully regenerated.[6] A downside, however, is the often poor biocompatibility, non-natural degradation products, and a loss of mechanical properties during degradation.[6] Due to these reasons, natural biomaterials like collagen are preferred in some cases over synthetic polymers as they are biodegradable and non-toxic. Of the natural polymers, exogenous collagen has been shown to be highly biocompatible and has been observed to have very weak antigenic properties.[6, 52]

Thermo-responsive inks

Almost all bioprinting techniques disperse the bio-ink through a nozzle onto the substrate. To obtain a clear image, the bio-ink should move through the nozzle easily but should become rigid upon dispersion. Thermo-responsive hydrogel inks have the advantageous property of tunability of their sol-gel state by changing the temperature.[53] Thermo-responsive polymers in these bio-inks consist of hydrophilic homopolymers or block copolymers that maintain a colloidal solution (sol) form at room temperature and form a gel at body temperature.[54] This allows easy, accurate printing in its sol state and a simple switch in temperature causes rapid gelation leading to high resolution printing.[53] Cells cultured on these thermo-responsive hydrogels form self-supporting sheets by producing their own extracellular matrix (ECM); the cell sheet can be detached from the substrate simply by reducing the temperature.[55] Naturally-derived thermo-responsive polymers have the advantage of being biocompatible, while synthetic polymers mostly have a higher mechanical strength. Both types of thermo-responsive polymers will be discussed below.

Natural and naturally-derived polymers

Gelatin is a collagen derivative that can be used in different bioprinting techniques, like extrusion-based,[56] piezo-electric inkjet,[57] and two-photon polymerization.[58] Gelatin itself has a random coil structure in solution and forms a helix below 35°C where helix-chain aggregation causes gelation.[53] To stop the liquification of gelatin above 35°C, it is most commonly modified with a methacrylate group, creating the photopolymer gelatin methacrylate (GelMa).[36, 59] Billiet *et al.* prepared photocrosslinkable GelMa interconnected porous constructs.[60] GelMa was used by Kolesky *et al*. to make ECM-like ink to support cells.[56] Both studies showed a high cell viability of over 95%. Gelatin naturally contains integrin-binding motifs, like arginine-glycine-aspartic acid (RGD), which allow cells to adhere and spread. Matrix metalloproteinase (MMP) sensitive degradation sites present in GelMa play an important role in the proliferation and migration of cells,[61] as MMPs cleave ECM components to allow cells to expand, reposition and proliferate.[62] Skardal *et al.* made use of the photocrosslinkable property of GelMa by co-crosslinking with methacrylated hyaluronic acid (HAMA) to yield an extrudable gel-like fluid for the two-step bioprinting of tubular constructs.[63] The bio-ink was biocompatible, allowed cell adhesion and cell proliferation, and showed no inflammatory response after subcutaneous injection into nude mice. The printed tubular construct contained viable cells that naturally secreted ECM to substitute the synthetic ECM environment. A printing method using gelatin called freeform reversible embedding of suspended hydrogels, or FRESH, was developed by Hinton *et al.*[64] In this technique, hydrogels are printed within a second hydrogel that is used as a support bath to improve print fidelity. This support bath consists of gelatin microparticles that act like a Bingham plastic, meaning that during printing the particles act like a fluid due to the high shear stresses but become rigid at the low shear stresses in the bath. Myoblasts in suspension printed with

FRESH showed a 99.7% viability. Although most articles using GelMa do not specify the type of GelMa used, gelatin comes in two types. Gelatin from acid treatment generates type A, while an alkali treatment will yield type B.[65] Lee *et al.* studied the characteristics of both types of GelMa as these influence the properties of GelMa and thus its printability. They showed a higher methacrylation of type B, although type A showed a higher resolution after extrusion printing. Both types of GelMa showed a cell viability of around 75% in cell-laden printed constructs.[65] Jia *et al*. designed a cell-responsive bio-ink by using GelMa combined with sodium alginate and 4-arm poly(ethylene glycol)-tetra-acrylate (PEGTA).[66] This bio-ink was firstly crosslinked ionically with calcium ions, followed by covalent photocrosslinking of the GelMa with PEGTA. Extrusion printing of the bio-ink created vascular constructs promoting cell adhesion, proliferation and migration with a cell viability exceeding 80%. Another GelMa blend was made by Kang *et al.*, who used GelMa in composition with poly(ethylene glycol) (PEG) diacrylate/alginate.[41] By testing different valve cell types and photo-initiators, they identified parameter combinations for high cell viabilities (93-95%). Decreased cell viabilities were found in photocrosslinked inks due to a higher general oxidative stress level and most possibly other stress mechanisms. An additional challenge lies in the design of bio-inks for cardiac tissue constructs. Electrical coupling between cells is crucial for a functional cardiac tissue. Zhu *et al.* therefore created a cytocompatible bio-ink with a conductive component and a cell viability of over 70% by incorporating gold nanorods (GNRs) into a GelMa-based bio-ink. Cetyltrimethylammonium bromide (CTAB)-coated commercial GNRs were coated with GelMa to improve biocompatibility, then were mixed with a solution of GelMa and photo-initiator to create a prepolymer bio-ink capable of printing synchronized contracting cardiac tissue.[67]

Collagen is part of the ECM that provides structural and biochemical support to the surrounding cells. Collagen types I, II, and III are found in hard and soft connective tissues. A collagen molecule consists of three polypeptide chains that each form a helical structure.[68] The chains contain RGD residues that form a motif able to adhere cells via integrin-RGD binding.[6] Collagen is a biodegradable protein with little toxicity and so it is a widely used material for bioprinting. As part of the ECM, collagen can provide stability to 3D printed tissues as a surrounding scaffold.[69] Lee *et al.* showed the potential of collagen for tissue engineering by creating a human skin model with collagen as representation of the dermal matrix with fibroblasts and keratinocytes showing cell viability of around 98%.[10] Skardal *et al.* combined fibrin and collagen in one bio-ink together with amniotic fluid-derived (AFS) cells or bone marrow-derived MSCs.[70] After deposition into skin wounds, the cell-containing bio-inks showed an increase of wound closure and angiogenesis compared to the control. The AFS cells showed the highest amount of angiogenesis which is probably caused by secretion of growth factors by these cells. Rhee *et al.* developed soft tissue implants with high-density collagen hydrogels loaded with meniscal fibrochondrocytes for load-bearing applications.[71] Cells had a viability of around 90% directly after printing and maintained a high viability over 10 days in culture. Kim *et al.* also studied the use of a genipin-crosslinked collagen-based hydrogel to produce a porous and mechanically strong construct.[72] Osteoblast-like cells and human adipose stem cells were combined with the collagen bio-ink to create a 3D construct with 95% cell viability and extensive cell proliferation. Collagen is also widely used as a biomaterial for wound healing, as a component of sponges, hydrogels, membranes, wound dressings, and in direct skin replacement. A collagen mimetic protein can even be used to anchor cytoactive agents in damaged tissue to promote wound healing.[73] Collagen can also be used in osteochondral tissue regeneration. Park *et al.* printed osteoblast-

encapsulated Col-1 hydrogels and chondrocyte-encapsulated HA hydrogels creating 3D osteochondral mimicking structures with a cell viability of more than 90% for both cell lines.[74] Shim *et al.* created an MSC-laden hydrogel consisting of two ECM materials, atelocollagen and HA, which enabled osteochondral tissue regeneration in the knee joints of rabbits.[75] The group of Cho used a collagen bio-ink containing three different cell types infused in a framework of poly(ε-caprolactone) (PCL) to create a 3D liver microenvironment. The printed structure contained a capillary-like network and showed hepatocyte growth with a viability of 92-99%, demonstrating the ability to create multicellular 3D liver constructs.[76]

Elastin is a protein that is present in elastic fibers, which can be found in tissues that need to be able to recover from deformation.[77] Elastin is formed from tropoelastin, the monomer of the elastin polymer. Each monomer consists of a hydrophobic domain (mostly valine, glycine, and proline) and a hydrophilic domain (mainly lysine and alanine).[78] Natural elastin is hard to extract, so a synthetic naturally inspired polymer is used. These elastin-like peptides (ELPs) are obtained by expression in *E. Coli* and purification of the cell lysates.[77] They are therefore also known as elastin-like recombinamers (ELRs).[79] Thermo-responsive inks can be created with ELRs as they undergo sol-gel transition at increased temperature. The random-coil ELRs hydrophobically fold into ordered β-spirals upon heating.[77]

Silk from the silkworm contains two proteins, sericin and fibroin. The fibroin part of silk can be used in hydrogels. Fibroin consists of a light and heavy chain bound by disulfide bonds and consists of a repeating pattern of Gly-Ser-Gly-Ala-Gly-Ala units. The fibroin of the silkworm is water-soluble and has a β-sheet conformation stabilized both by hydrogen bonding and van der Waals interactions between hydrophobic side chains.[80, 81] To obtain a water-soluble form, the strong hydrogen bonds

need to be broken.[77] After dialysis, the fibroin has a random-coil conformation that can undergo a sol-gel transition by forming β-sheets.[82] The gelation conditions of fibroin are mild and therefore suited for cell encapsulation. Very recently, Qi *et al.* published a review that summarizes various constructions of silk fibroin-based materials.[83] Only two recent publications will be discussed below. Das *et al.* created a silk fibroin-gelatin bio-ink with encapsulated nasal inferior turbinate tissue-derived mesenchymal progenitor cells.[84] Gelation could be controlled temporally by enzymatic and physical crosslinking. Optimization of different levels allowed the creation of 3D tissue constructs with a high cell viability directly after printing (~96%) and after 30 days of culture (~86%). The encapsulated stem cells showed multilineage differentiation to specific tissue over a 3 week culture study. Rodriguez *et al.* developed a silk-based ink in combination with gelatin as bulking agent and glycerol for physical crosslinking.[85] The printed soft tissue resembling constructs remained intact up to three months, showed biocompatibility and promoted cellular infiltration and tissue integration. The optimal conditions of the ink included a minimum gelatin concentration of 10% w/v and a 1:1 ratio of silk to gelatin. Minimal inflammatory response was observed in a mouse model.

Fibrin is a hemostatic agent used as a sealant in surgery. It has excellent biocompatibility, promotes cell attachment, and causes minimal inflammation and foreign body reactions.[6] Fibrin gels are formed by the polymerization of fibrinogen monomers that is catalyzed by a thrombin solution. Depending on composition and ionic strength, their mechanical properties, gelation time, degradation time, and stability can be controlled.[6] Fibrin can be used for wound healing as the fibrin network enables blood clotting by a crosslinking process preventing bleeding.[86] The cell attachment property of fibrin promotes a high cell seeding efficiency and uniform cell distribution, however it suffers from long-term stability problems. Cui *et al*. created micro-capillaries by bioprinting human dermal

microvascular endothelial cells (HMVECs)-laden thrombin and a calcium solution on a fibrinogen substrate. The HMVECs then formed a capillary network after 21 culture days.[87] Neural constructs can also be created by printing neural cells on fibrin.[88] An *in vitro* study produced a printed urethra consisting of a PCL and PLCL scaffold and fibrin hydrogel. The printed structure containing urothelial cells and smooth muscle cells maintained a cell viability of over 80% over 7 days post-printing[citation].[89]

Alginate is a naturally occurring polysaccharide that is biocompatible, biodegradable and has a low toxicity.[6] Alginate can crosslink through its polymeric backbone, which contains negatively charged carboxylate groups that can interact with positively charged calcium cations, yielding a crosslinked network.[5] Alginate can be covalently crosslinked by reacting with poly(ethylene glycol)-diamines, or cross-linked by phase transition.[90] Alginate can also form a hydrogel by interaction with cells. Alginate modified with cell adhesion ligands can bind with cells to form a reversible, long-distance network without chemical agents. These properties allow alginate and its derivatives to be used in various biomedical applications, like regenerative medicine, tissue engineering, and drug delivery. Munguia-Lopez *et al.* created a hydrogel composed of alginate, gelatin and carbon nanotubes (CNTs) to create bio-ink with tunable properties for a broad range of applications. An extrusion-based printer deposited the new bio-ink, yielding a highly porous material with a well-distributed layer of cells.[91] Alginate can also be used in bone tissue engineering. Torres *et al.* tested the behavior of osteoblasts on β-tricalcium phosphate-hydroxyapatite scaffolds coated with alginate. The osteoblasts were able to adhere and proliferate on these scaffolds with a cell viability of approximately 100%.[92] Park *et al.* studied different compositions of high MW alginate (High Alg) and low MW alginate (Low Alg).[93] They showed the successful construction of 3D scaffolds for 3 wt% High Alg and 1:2 Low Alg to

High Alg compositions. Constructs printed with fibroblasts showed high cell viability (~100%) and growth up to 7 days of culture. An alginate bio-ink was used by Xiong *et al.* to test the feasibility of gelatin as an energy absorbing layer in LIFT. An increased cell viability of 80% after printing compared to the control viability of 77% was observed.[94]

Hyaluronic acid (HA) is a hydrophilic linear anionic polysaccharide composed of 1,3-β-D-glucuronic acid and 1,4-β-*N*-acetyl-D-glucosamine.[95] It can be found in most connective tissues in all living organisms. Currently, HA is used as a lubricant and in healthcare by preventing post-surgical adhesions.[96] HA can only form a hydrogel when modified through esterification of the carboxyl or hydroxyl group and cross-linking.[97] It is commonly modified with methacrylate groups which allows photocrosslinking.[77] As HA is naturally present in tissues, it can be used to encapsulate cells. Ouyang *et al.* created a dual-cross-linking hydrogel using HA in combination with host-guest chemistry.[98] Adamantane was used as the guest and coupled to HA. The host, β-cyclodextrin, was separately coupled to HA. Both macromolecules were functionalized with methacrylate groups to enable photocrosslinking for a stronger gel. A shear-thinning hydrogel was created that is able to self-heal due to the employed host-guest chemistry. Host-guest chemistry allowed rapid stabilization straight after extrusion printing. Covalent photocrosslinking after printing increased stability to create a hydrogel stable up to one month. Further modifications can be made to the HA backbone, for instance, RGD was implemented to support cell adhesion. Very recently, Poldervaart *et al.* produced a hydrogel with increased storage and elastic moduli by UV irradiation of methacrylated HA.[99] MSCs seeded within the hydrogel were able undergo osteogenic differentiation and maintained a cell viability of 64.4% over 3 weeks.

The natural polysaccharide agarose has a comparable gelation mechanism to gelatin.[53] Its random coils transform into a double helix conformation when temperature reaches 30-40°C. Bertanossi *et al.* used fibres of agarose to create a vascular network within hydrogels. Endothelial cells were subsequently successfully infiltrated within the created micro-channels.[100] A hybrid approach consisting of poly(D,L-lactic-co-glycolic acid) (PLGA) porous microspheres containing mouse fibroblasts and an agarose-collagen hydrogel was created by Tan *et al.*[101] (Figure 5). The porous microspheres increased cell adhesion and proliferation before printing, while the use of collagen within the agarose hydrogel improved cell affinity and migration. After one and two weeks of culture, cells showed a viability of over 90%. Agarose can also be used in cartilage tissue engineering. Daly *et al.* tested four different hydrogels, namely agarose, alginate, GelMa and a commercially available PEG-methacrylate-based hydrogel (BioINK™), on their printing properties and their capacity to support mesenchymal stem cells (MSCs) in their *in vitro* development to hyaline cartilage or fibrocartilage.[102] All bio-inks showed a high cell viability post-printing (~80%). Agarose and alginate showed development of hyaline cartilage-like tissue, while GelMa and BioINK™ showed fibrocartilage-like tissue development. Gu *et al.* presented a bio-ink for the direct-write printing of human neural stem cells composed of alginate, carboxymethyl-chitosan (CMC), and agarose. The designed bio-ink undergoes rapid gelation through crosslinking, and forms a stable porous 3D neural mini-tissue construct.[103] The cells were encapsulated by post-printing gelation giving a cell survival of around 75% directly after printing. The overall gel stiffness lies in the required range for brain tissue, and a porous and permeable gel that enhanced cell survival was obtained. This approach enables the characterization of neural cells during the study of neural development and function.

Carrageenan is a water-soluble polysaccharide consisting of β- and α-D-galactose.[77] The amount of sulfate groups and their position determine the carrageenan family group.[104] Only κ- and ι-carrageenan form reversible hydrogels in the presence of cations through the transition from random-coil to a double helix.[105] The κ-carrageenan hydrogels are harder and less deformable than those from ι-carrageenan.[106] Unfortunately, this polysaccharide is not biodegradable, making it an unfavorable material for *in vivo* applications.[77] A thermo-responsive ink was made by Bakarich *et al.* through a synergistic crosslinking system consisting of κ-carrageenan, calcium ions, Jeffamine (poly(oxyalkylene amine)) and PEG diglycidyl ether to form κ-carrageenan/epoxy-amine ionic-covalent entanglement (ICE) hydrogels.[107] The extrusion printed ink undergoes gelation upon a change in temperature as the κ-carrageenan forms a double helix. The single sulfate group on each κ-carrageenan repeating unit is crosslinked by calcium; the resulting network is entangled with the epoxy-amine polymer to form a tough reversible hydrogel.

Methyl cellulose (MC), a derivative of the naturally occurring polysaccharide cellulose, is mostly used in pneumatic extrusion printers.[14] Above the lower critical solution temperature (LCST), hydrophobic interactions within the MC chain become dominant, creating a network.[108] The LCST of MC lies between 40-50°C. With the human body temperature at 37°C, MC can be used as a supporting material in tissue engineering.[53] For instance, Fedorovich *et al.* made a 4% (w/v) MC hydrogel containing bone marrow stromal cells (BMSCs) to test 3D fiber deposition by the Bioplotter system with an overall cell viability of 80% post-printing.[14]

The linear anionic polysaccharide gellan gum is composed of tetrasaccharide repeating units.[109] Two forms exist that both transform from random-coils to double-helices upon cooling. The acetylated isoform forms soft gels, while the deacetylated one forms hard gels.[110] The negatively

charged carboxyl side groups stop gel formation as the charges repel each other. Addition of cations allows shielding of the negative charges allowing gelation.[77] The presence of the carboxyl groups can provide additional properties. When modified with methacrylate, the hydrogel becomes photocrosslinkable increasing stability.[111] Lozano *et al.* used a gellan gum modified with RGD and combined with primary cortical neurons to form a bio-ink. This ink was used to print 3D brain-like structures with a cell viability of between 65 and 83% after printing. Modification with RGD increased cell proliferation and network formation.[34]

Recently, Mueller *et al.* created a bio-ink for cartilage bioprinting based on alginate sulfate combined with nanocellulose to obtain rheological properties suitable for printing.[112] The chondrocytes within the alginate sulfate-nanocellulose bio-ink showed cell migration, proliferation, and synthesis of the joint cartilage peptide collagen II before printing. After printing, performance was highly dependent on the nozzle geometry. Low extrusion pressure and shear stress produced migrating cells, but decreased cell proliferation. Conical needles with a wide diameter provided 3D structures with high shape fidelity and cell viability (>90%).

Synthetic polymers

Pluronics are ABA triblock copolymers consisting of hydrophilic PEG as the A block and hydrophobic polypropylene glycol (PPG) as the B block. Pluronic is a trademark poloxamer with many types that are mostly named with a letter followed by two or three digits. The letter stands for the physical state of the compound at room temperature; L for liquid, P for paste, and F for flake. The digits following this letter indicate the length and molecular weight (MW) of the Pluronic. The first one or two digits multiplied by 300 indicates the approximate MW of the hydrophobic block. The last digit

represents the PEG percentage in ten-fold. For instance, Pluronic F127, which is highly used in bioprinting, is a flaky solid at room temperature with a MW of approximately 3600 g/mol and 70% PEG content.[53, 56] Block copolymers like Pluronic form micelles in solution when the temperature dependent critical micelle concentration (cmc) is reached. Below cmc, Pluronics occur as single chains in solution. When the concentration increases the hydrophobic blocks aggregate as a core creating a micelle at cmc. The packing of micelles causes the solution to undergo a phase transition to a gel, but also leads to a gel with poor mechanical strength. The cmc has an impact on the printability of Pluronics. Depending on the Pluronic used, concentration and temperature should be varied. Pluronic F127 requires a minimum of 20% w/v for gelation and is mostly extrusion- or valve-based printed at 25-40% w/v.[14, 113] The advantageous gelation temperature and good printability make Pluronics suitable for 3D printing. Because Pluronic is a synthetic polymer it shows no bioactivity and cannot be used for systems where long-term cell viability is needed.[53] In 3D bioprinting it can therefore be used as a sacrificial layer.[114] Gioffredi *et al.* characterized different Pluronic F127 hydrogels to select the optimal composition for bioprinting.[115] Balb/3T3 fibroblasts loaded into the resulting bio-ink showed no decrease in cell viability after a 1 h printing session. To improve long-term cell viability and mechanical strength in Pluronic F127 hydrogels, Gioffredi *et al.* propose different options including coprinting with stabilizing agents. Pluronic F127 can also be used as a model ink to test mathematical models designed to improve printing resolution. Suntornnond *et al.* created a mathematical model for pneumatic extrusion-based bioprinting which they tested with Pluronic F127, which showed good agreement between experimental data and model predictions.[116]

PEG can be used in different compositions for 3D bioprinting.[53] It can be functionalized with diacrylate or dimethacrylate groups to create a photocrosslinkable polymer, and can be used to

fabricate hydrogels. Although there are few reports on printed PEG block copolymers, PEG is widely used as a crosslinker. PEG was used in combination with nanoclay by Hong *et al.* to create PEG-alginate-nanoclay hydrogels with cell viability ranging from 75.5% to 86.0% over a 7 day culture period.[117] The properties of each component resulted in a highly stretchable and tough hydrogel that could be used to create complex 3D structures. Censi *et al.* created a hydrogel by thermal gelation of an ABA triblock copolymer consisting of partially methacrylated poly(N-(2-hydroxypropyl)methacrylamide lactate) and PEG, with the latter being the B block. For extra stability, the polymers where crosslinked by photopolymerization of the methacrylate groups. Encapsulated chondrocytes showed cell viabilities of ~94% and ~85% after 1 and 3 days, respectively.[118] Very recently, Tseng *et al.* used PEG diacrylate (PEGDA) in a glucose-sensitive self-healing hydrogel to create vascularized constructs.[119] A glucose-sensitive hydrogel composed of PEGDA plus dithiothreitol crosslinked with borax was used as a sacrificial material. To create the construct, a pattern of the PEGDA-dithiothreitol-borax hydrogel was embedded into a non glucose-sensitive hydrogel containing neural stem cells. By immersion into the glucose-containing culture medium, the sacrificial hydrogel was removed from the construct and a tubular channel was formed in the neural stem cell-containing hydrogel (Figure 6). Perfusion of vascular endothelial cells in the lumen of the channels covered the non-sacrificial hydrogel after migration and alignment after 3 days. A capillary-like structure was visible after 14 days.

Another type of synthetic polymer used in 3D bioprinting is poly(N-isopropylacrylamide) (PNIPAAM),[53] which has a gelation temperature of 30-37°C. In this temperature range, the PNIPAAM chains undergo a coil-globule transition and become hydrophobic; gelation occurs through hydrophobic interactions between these chains.[120] To improve biocompatibility, PNIPAAM is mostly

combined with HA or alginate. Kesti *et al.* combined HA-PNIPAAM with HAMA to create high resolution scaffolds with high viability of bovine chondrocytes of 80% 3 hours post-printing and 97% after 4 days.[31]

Poly(organophosphazenes) are synthetic polymers with a backbone of alternating nitrogen and phosphorus atoms with two organic side groups on almost all phosphorus atoms. The general formula is $(N=PR_1R_2)_n$, where R_1 and R_2 represent the side groups.[121] When the side groups are oligo-ethyleneoxy groups, poly(organophosphazenes) can form biocompatible thermally responsive hydrogels that can be crosslinked through gamma-irradiation. Ionic crosslinks can be formed when oligo-ethyleneoxy and carboxyphenoxy side groups come in contact with di- or tri-valent cations.[122] In conjugation with RGD, poly(organophosphazene) can be used to support MSC differentiation into osteogenic cell lines. Chun *et al.* covalently linked GRGDS to carboxylic acid-terminated poly(organophosphazene).[123] Due to the liquid state of the conjugates at room temperature, the liquid could be injected in combination with rabbit MSCs into nude mice. At body temperature the conjugates formed a hydrogel. Osteogenesis markers increased and showed initiation of the maturation process after 4 weeks, indicating the promising use of the poly(organophosphazene)-GRGDS conjugates in bone tissue engineering. In 2010, Park *et al.* made use of the injectability of poly(organophosphazene) to develop a protein release system. Protein diffusion was controlled by the incorporation of polyelectrolyte complexes (PECs) which formed electrostatic interactions with the proteins. The protein diffusion was dependent on the PECs, gel viscosity, and weight ratios of polycations and proteins. Overall, Park *et al.* showed the potential of the PEC-poly(organophosphazene) hydrogel as a protein delivery system.[124] A few years later the same group used the same system in combination with protamine sulfate to control the delivery of human growth

factor in rats.[125] An increased growth rate was observed for the hydrogel in combination with daily injections of the growth factor for 7 days. Huang *et al.* included α-cyclodextrin (αCD) into mixed-substituted polyphosphazenes to create a mechanically strong hydrogel for scaffold material by host-guest chemistry and photocrosslinking.[126] Polyphosphazene was substituted with either glycine ethyl ester groups (GlyEE) to promote cell affinity and biocompatibility, or acrylate-terminated PEG groups (PEGac) for self-assembly in the presence of αCD and preventing cell adhesion. After UV irradiation, a mechanically strong gel was formed with a high stability in water. By tuning the ratio GlyEE:PEGac the hydrogel could be tuned from cell-philic to cell-phobic. Due to the biocompatible nature and rapid sol-gel transition of poly(organophosphazenes) they could be a promising group of materials for 3D bioprinting.

Photocrosslinkable inks

Crosslinking of inks enables a low viscosity solution with low shear stress during printing to protect cells and create a high resolution printable structure. To be able to do this, the polymers in the ink must be crosslinked quickly and be compatible with the emitted wavelength of the laser source.[127] Ouyang *et al.* introduced a new method to allow a longer crosslinking time with photocrosslinkable inks that do not polymerize fast enough for current approaches. They proposed a printing technique called “in-situ-crosslinking” in which a photo-permeable capillary was used to crosslink the ink seconds before deposition (Figure 7).[128] To test their hypothesis, Ouyang *et al.* tested five photocrosslinkable inks: HAMA, GelMa, PEGDA and norbornene-functionalized HA (NorHA), which were UV-crosslinked with Irgacure 2959; and NorHA plus the photoinitiator lithium phenyl-2,4,6-trimethylbenzoylphosphinate (LAP) and visible light. The new in-situ-crosslinking technique allowed

printing of high resolution structures with high cell viability from photocrosslinkable hydrogels, independent of ink viscosity.

Microcarriers

Microcarrier technology in combination with bioprinting allows cells to expand extensively while forming multi-cellular aggregates. Microcarriers also allow phenotypic control of the seeded cells.[129] They do this by serving as substrates for anchorage-dependent cells.[130] The materials used for these microcarriers can either be synthetic polymers, glass, or natural polymers such as cellulose, gelatin, or collagen. Due to their porous spherical morphology, cells can attach to the microcarrier surface and proliferate.[16] The porous morphology also improves the transfer of gasses and nutrients, and allows a larger surface area for cell attachment.[130] Levato *et al.* created a bio-ink containing MSC-laden poly(lactic acid) microcarriers encapsulated in GelMa-gellan gum.[129] The microcarrier-loaded printed structures had an increased compressive modulus and showed a high cell density, viability (60-90%), cell adhesion, and osteogenic differentiation of the MSCs. The high microcarrier concentration in the GelMa-ink did not compromise the printability of the bio-ink. Jakob *et al.* developed a microcarrier-based 3D culture model of the epithelium.[131] The microcarriers were porous Sephadex beads coated with denatured type I collagen to represent the epithelial basal lamella (Cytodex 3 beads), enabling cells to attach through integrins and other transmembrane receptors. A fibroin microcarrier was used by Goncharenko *et al.* to study the influence of 3D culture and mineralization on osteoblast differentiation and actin skeleton reorganization.[132] Mineralization and the use of fibroin microcarriers increased the expression of the osteogenesis marker alkaline phosphatase and changed the morphology of the actin filaments.

Cell aggregates

Cell aggregate configurations form a scaffold-free alternative for bio-inks. Cell-cell interactions are of crucial importance in tissue formation. The type-I transmembrane protein cadherin causes multicellular aggregates for tissue morphogenesis.[133] Cadherin allows intercellular adhesion which is important for cell-cell communication.[16]

Tissue spheroids

Tissue spheroids are spherical cell aggregates, generally 200-400 µm in diameter. They can be used as building blocks for tissue engineering or as tissue models for pharmaceutics.[16] The self-assembling cellular spheroids mimic developing tissue through fusion and reorganization.[134] Most cells do not spontaneously aggregate in culture, rather they have to be induced to aggregate by some means. Different techniques exist for the generation of tissue spheroids, the most common of which uses cell-adhesion inert hydrogel moulds in which thousands to millions of cells are cultured in micro-wells for 24-28 hours.[16] At the bottom of the well, cells adhere to each other and form spheroids due to radial contraction and cadherin-mediated cytoskeletal reorganization.[135] The hanging drop method uses gravity to concentrate the cells in one spot for cell aggregation. It is a simple technique that only requires a tissue culture plate and a cell suspension. A small drop of the cell suspension is pipetted on the plate, which is then inverted to make the droplet hang.[136] Another technique uses a U-shaped trap of polydimethylsiloxane (PDMS) connected to a perfusion channel. Cells entrapped in the U-shape aggregate and are not prone to necrosis due to the flow of media and oxygen. It is, however, difficult to extract intact cell aggregates from the PDMS.[16] Guo *et al.* recently used acoustic waves to assemble

cells on a membrane.[137] The liquid overlay technique was used by Metzger *et al.* to generate tissue spheroids from fibroblasts and/or osteoblasts.[138] They studied the cell-surface interaction between the spheroids and artificial ECMs. The artificial ECMs consisted of sulfated hyaluronan that was co-fibrillised with collagen. The spheroid size changed depending on the sulfate level and the cell type, showing the usage of tissue spheroids for studies of cell-surface interactions. Magnetic 3D bioprinting was used by Tseng *et al.* to validate 3T3 fibroblast spheroid contraction in response to toxic compounds. Spheroid contraction assays could be used for the high-throughput screening of compounds in a 3D environment.[139]

Cell pellets

Cell pellets can be generated by centrifugal or gravitational forces. Generally, cell viability decreases after 24 hours due to a limited flow of medium and oxygen.[16] The cell pellet can be transferred to a mould to improve cohesion through intercellular interactions. Cell pellets are mainly used in extrusion-based printing. Owens *et al.* bioprinted fully biological grafts to bridge nerve ends after nerve rupture.[25] Cell pellets were used to form cellular cylinders that were deposited by a bioprinter into a support structure. Another bio-ink containing pellets of mouse embryonic fibroblasts was fabricated and used to create a scaffold-free macro-vascular structure for aortic tissue regeneration.[140]

Tissue strands

Tissue strands are cylindrical mini-tissues that can be used to produce tissue through bioprinting approaches. Akkouch *et al.* presented a method to scale-up the fabrication of tissue

strands with a cell viability of up to 94% 7 days after printing.[135] Semi-permeable tubular alginate capsules were used to allow exchange between cells and the medium for nutrients and oxygen supply. Alginate capsules were extrusion-printed through coaxial printing of sodium alginate and a crosslinker solution. Cell pellets were injected into the alginate capsule till the capsule was tightly filled. The ends of the capsule were blocked during 5-7 days of culture for the aggregation of cells. The alginate capsule was then decrosslinked leaving the tissue strand. A heterocellular tissue strand could be fabricated through an overnight co-culture with a secondary cell type and fibronectin. Yu *et al.* presented a new method to print tissue strands without the need for a liquid delivery medium or moulding structure, giving a cell viability of 75% after printing, recovering to 87% after 7 days.[45] Tissue strands as presented by Akkouch *et al.* were loaded into a unique print-head to rapidly fabricate tissue constructs. Cells used in this study were chondrocytes, which are known to prefer hypoxic conditions.[141] Whether tissue strands with their low oxygen level in the core of the strand can be used for other tissue constructs needs to be explored. Yu *et al.* however, showed the use of tissue strands for cartilage formation.[45]

Decellularized matrix components

The protein composition of the ECM varies depending on the tissue it needs to support on a physical, chemical, structural, and biological level. The ECM can be harvested from various tissues and decellularized by extensive washing with surfactant, yielding a protein mixture for use as a bio-ink. It is important to use ECM from the tissue type that is intended to be recreated, as each ECM has different functionalities for each tissue.[6] The dECM can be harvested from tissues like skin, adipose tissue,[142] cartilage,[143] bone and heart.[144, 145] The microenvironment is important for cellular differentiation and

function, therefore it is important that the dECM has the same properties as the ECM before decellularization. Singh et al. showed that a common decellularization protocol involving trypsin resulted in a severe loss of mechanical stiffness and collapse of the collagen architecture, leading to a decrease of porosity.[146] Jang *et al.* were able to tailor the mechanical properties of dECM by photocrosslinking with vitamin B2. The resulting structures showed high viability (≥95%) and proliferation of cardiac progenitor cells.[147] For harder material tissues, like bone and cartilage, ceramic materials or composite scaffolds are still needed to generate a mechanically stable scaffold.[148]

APPLICATIONS

Tissue engineering and regenerative medicine

With donor numbers declining there is a need for tissue engineering and regenerative medicine to fill the void. Several tissues have already been explored for 3D bioprinting, including the heart valve, myocardial tissue, blood vessels, and musculo-skeletal tissues. For these tissues to be successful they have to provide the proper environment to allow cell proliferation and differentiation. Their elasticity, flexibility and recovery rate need to mimic that of the native tissue environment.[18]

Hard tissue engineering mostly focusses on creating bone and cartilage tissues for aging diseases and the musculoskeletal system.[4] Scaffolds, which mostly consist of polymers, ceramics and hydrogels, are commonly used to allow tissue regeneration. Yu *et al.*, however, were able to generate a scaffold-free structure using scalable tissue strands as a bio-ink for articular cartilage tissue.[45] Gao *et al.* examined the ability of HA and bioactive glass (BG) nanoparticles to stimulate MSCs osteogenesis in a scaffold of PEG-dimethacrylate (DMA).[149] The scaffold mixture was co-printed with HA and BG on a thermal inkjet printer. Both substances were polymerized simultaneously to achieve a highly

accurate placement. The scaffold containing HA showed the highest cell viability and improved mechanical characteristics. Kelly's group used an MSC-laden bio-ink and a PCL network to create templates with decoupled biological and mechanical functionality. They were able to fabricate a vertebral body with functional vasculature, and trabecular-like bone with a supporting marrow cavity.[46]

A great challenge in tissue engineering lies in the fabrication of cardiac tissues, due to the hierarchical structure of the myocardium and the need for angiogenesis. Zhang *et al.* created an endothelialized-myocardium-on-a-chip by combining bioprinting, microfluidics, and stem cells.[59] Using a composite bio-ink, endothelial cells were printed together with a hydrogel to cover the inside of microfibers with endothelial cells. Cardiomyocytes were then seeded on the endothelial layer, generating a spontaneous and synchronous contracting myocardium.

To study the properties of neural networks and pathogenesis of neurological diseases, artificial neural tissues are engineered. Lee *et al.* patterned a multi-layered collagen gel with rat embryonic neurons to generate a flexible tool for artificial neural tissue.[150] A year later, the same group constructed an artificial neural tissue of a vascular endothelial growth factor-releasing fibrin gel, collagen hydrogel, and murine neural stem cells.[151] They showed migration of cells only occurred in the growth factor-containing cells compared to the controls.

Transplantation and clinical applications

Tissue engineering has been able to create multiple tissue types as *in vitro* models and for regenerative medicine applications. With the severe problem of tissue rejection after transplantation, 3D bioprinting can assist by creating personalized tissues. The field has already been able to create

vascularized tissues, a challenge that still needs to be explored further. For personalized tissue transplants, 3D bioprinted structures need to resemble native tissues perfectly. DBB is a technique that can be used for the deposition of the bio-ink directly into the wound during surgery as it does not require contact and does not bear toxic or unsafe interventions.[5] At this point, bioprinting cannot yet be used for human use. However, 3D printing has been used to treat the life-threatening condition of tracheobronchomalacia in an infant.[152] Tracheobronchomalacia is a rare disease leading to the collapse of the central airways and respiratory insufficiency. After FDA approval and a written consent of the patient's parents, Zopf *et al*. created a biodegradable airway splint out of PCL with a laser-induced forward transfer printer. One year after the implantation of the customized tracheal splint, imaging showed a solid left mainstem bronchus without any complications. The splint is expected to be resorbed fully after 3 years. This procedure showed the possibilities for the combination of high-resolution imaging, computer-aided design, and 3D bioprinting for personalized transplantation and clinical applications.

The ability of 3D printed constructs to direct tissue formation *in vivo* was also shown by Cooper *et al.*[153] They demonstrated osteoblastic differentiation according to a bone morphogenetic protein-2 (BMP-2) pattern *in vitro* and subsequent bone formation *in vivo*. In another *in vivo* study, Mooney *et al.* developed a polymeric system for the delivery of multiple growth factors for the development of tissues and organs.[154] The generated system is able to deliver two or more growth factors, with a controlled dose and release mechanism. They demonstrated their system by delivering two growth factors for vascular development, leading to a mature vascular network *in vivo*.

Very recently, Jeon *et al.* were able to print hepatic 3D structures using alginate. They cultured human liver cancer cells (HepG2) on the alginate structure to test the feasibility of 3D bioprinting for

liver tissues. Extensive growth on the 3D model was observed compared to the 2D culture and structural aspects of the liver were exhibited better.[155] Multiple studies have shown the great potential of 3D bioprinting for transplantation and clinical applications. As 3D bioprinting has many application areas, the FDA has provided guidance for its implementation in biomedical device manufacture.[156] Another recent study included the 3D bioprinting of skin constructs for burn injuries. Cubo *et al.* printed human bilayered skin by using a bio-ink consisting of human plasma, primary human fibroblasts and keratinocytes obtained from skin biopsies.[157] The printed construct has already been used to treat skin wounds of patients in Spain. They were able to create 100 cm^2 of bilayered skin within 35 minutes. The printed constructs were indistinguishable from bilayered dermo-epidermal equivalents.

Drug testing and high-throughput screening

The drug development process is extremely costly and it takes around ten years before a new drug gets regulatory approval. The approved drug is the only one of around 10,000 initial candidates that passes through all stages of the screening and regulatory process. Of all the drug candidates that make it to clinical trials, only one out of ten gets market approval.[158] Failure of drug candidates in clinical trials can be caused by several reasons; low efficacy, toxicity, and adverse events, to name a few.[159] Currently, drugs are tested in 2D cell culture formats, followed by animal testing and clinical trials. 2D cell cultures do not represent the complex 3D nature of human tissues, making them non-predictive and unreliable.[160] 3D cell culture platforms together with perfusion culture technologies are creating more representative and predictive models of the behaviour of cells *in vivo*. A reliable human model is

needed to make drug discovery less costly and quicker. This model has to dismiss ineffective and toxic compounds as soon as possible.

3D bioprinting is able to generate 3D models containing human cells to create a microenvironment that most closely resembles the native environment, and facilitates cell-cell and cell-matrix interactions.[161] These allow high-throughput screening of compounds to accelerate the drug discovery process. Li *et al.* created a 96 micro-scaffold array on a chip that enabled high throughput 3D cell culture, drug administration and quantitative *in situ* assays.[162] Their microarray allows fast manual loading and with a total medium consumption in the microliter range. The group of Marsano created a clinically compatible fibrin/HA scaffold seeded with nasal chondrocytes that were functionalized with the FDA-approved drug bevacizumab to block vascular growth.[163] Bevacizumab is known to sequestrate vascular endothelial growth factor from its environment. These scaffolds were able to block vessel in-growth in the host and enhanced the constructs' survival rate by four-fold.

Cancer research

The ability of 3D bioprinting to mimic the native environment can also be used in the study of cancer pathogenesis and metastasis. The DBB technology can fabricate high-resolution tissue models with great repeatability.[5] Xu *et al.* used DBB to build a 3D model for the investigation of multiple unknown regulatory feedback mechanisms between tumour and stromal cells.[164] To do so, Matrigel was overlaid with human ovarian cancer cells, which spontaneously formed multicellular aggregates (acini). The group of Zhang investigated a model for breast cancer metastasis.[165] Bone is one of the primary sites where breast cancer metastasis occurs. Zhang *et al.* therefore developed a biomimetic bone matrix using stereolithography. Matrices consisted of osteoblasts or MSCs encapsulated in

nanocrystalline HA. Breast cancer cells were seeded on the matrices, enabling the study of their interaction. Breast cancer cells secreted more vascular endothelial growth factor compared to the control and the presence of the matrix cells enhanced their growth, while the cancer cells decreased the matrix cells proliferation.

LIMITATIONS AND FUTURE PERSPECTIVES

3D bioprinting has gained much interest in recent years, leading to a huge increase in the number of publications in the area. New technologies have been invented to overcome challenges set by other methods, and new improved approaches will be proposed in the future. The field is still at an early stage and there are still many challenges that need to be faced. One such challenge is the construction of whole organs. Organs are complex structures that need multiple cell types to be co-located, as well as sufficient mechanical strength to maintain shape and integrity.[18] Printing resolution needs to be improved to fabricate structures with a complex inner architecture and 3D printed structures need to be implemented with a vascular network.

Previous studies have generated vascular networks *in vitro*[87] and *in vivo*.[154] In 2011, Fedorovich *et al.* used endothelial progenitor cells (EPCs) and multipotent stromal cells to generate a heterogenous scaffold.[8] While the multipotent stromal cells differentiated into a bone-like structure, the EPC layer allowed the formation of blood vessels. Different strategies have been used to improve vascularization since then; Yu *et al.* were able to create alginate-based well-defined vasculatures using human umbilical vein endothelial cells.[166] They showed the ability of this vascular network to promote tissue maturation inside, but also to support the fibroblastic tissue self-assembly around it. Despite this promising progress, further improvement is still needed, as scaffold-free vascularization attempts

have been difficult to scale-up.[24] A 3D printed structure of greater than 1 cm thickness, consisting of multiple cell types, was vascularized by Kolesky *et al.*[167] This structure maintained its integrity and viability on a chip for more than six weeks. To achieve this, co-printing techniques were used to integrate parenchyma, stroma and endothelium into one structure.

Some challenges lie in the key components of bioprinting, namely the bioprinter and the bio-ink. The different forms of DBB all use a print-head to deposit a bio-ink. To create a technique that can print high resolution tissues with an even amount of cells, the droplet volume, the placement of these droplets, and the number of cells encapsulated in a droplet need to be controlled.[5] Components need to be tuned to optimise the rheological properties of the bio-ink to allow precise printing whilst protecting the cells against shear forces, even at high cell concentrations. To be able to use bio-inks with viscosities for printing at sub-micrometre to micrometre resolution, the nozzle geometry needs to be altered as this restricts bio-ink viscosity and droplet size.[5] Furthermore, bioprinted tissues and organs require further testing on their long-term stability and reliability. To overcome the restrictions of current print-heads and nozzles, new techniques have to be introduced.[5]

An important component of a bio-ink are the cells, which need to be cultured in large amounts to be used for transplantation applications. The process to generate these can take weeks to months for each cell type.[5] As human organs and tissues contain various types of cells,[168] different cell types need to be cultured for a single organ or tissue. An advantage of bioprinting is the short time needed to print a structure, which should not be held back by the generation of its materials. Therefore, a technique needs to be developed to accelerate cell expansion times without harming the cells or increasing mutations.[5]

The post-printed structure needs to develop to a functional tissue construct gradually and successfully.[4] Key factors to achieve a functional tissue construct are the cell response, stability of the printed structure, and ECM deposition.[169] The microenvironment created by the ECM needs to allow differentiation and proliferation of the printed cells. To enable the ECM to guide stem cell differentiation, new materials need to be created to allow the ECM to send out signalling cues. As the biomimetic materials have to degrade to give way to the body's own ECM, this degradation needs to be controlled to ensure the synthetic ECM is not degraded too rapidly or too slowly.[134] The matrix component materials are also very important; they should support cell growth and create a substrate with mechanical and physical properties matching that of the native environment. New materials and printing mechanisms need to be developed to enable specific matrix phenotypes after bioprinting.[170]

The mechanical strength of current synthetic ECMs, especially hydrogels, is weak. To strengthen the mechanical properties of hydrogels they can be co-printed with degradable and biocompatible support materials.[5] To construct viable, large area and mechanically strong tissues, a capillary network needs to be implemented. Lee *et al.* used natural cellular mechanisms to overcome this problem.[171] They created a microvascular bed between two large fluidic vessels, which were connected by angiogenic sprouting through a natural maturation process. Combining of support materials and vascular networks will provide the opportunity to create print heads with an extremely small nozzle orifice diameter.[5]

For the mechanical strength of matrix components to be increased, fabrication time needs to decrease so that crosslinking can be induced sooner. However, shear stress is generated between the interior of the nozzle and the bio-ink components, including the cells.[18] This induces cell damage which will increase with a decreasing fabrication time. Time is thus an important parameter in 3D

bioprinting. Consequently, 4D bioprinting, which allows 3D printed structures to change shape and functionality over time on application of an external stimulus, is becoming a key area of research.[172] This technique is expected to broaden the field of 3D bioprinting.

Many advances have occurred which will accelerate the future fabrication of functional human organs. Although the routine transplantation of tissues and organs is still some way ahead, other applications of 3D bioprinting can already be considered, for example the production of human tissue-based models. This has opened the door to improved drug discovery and disease modelling. By using human induced-pluripotent stem cells derived from various patient groups, organ-on-a-chip models are enabled to take genetic variation into account for drug discovery.[5] Furthermore, the tissue models and microarrays presented introduced science to a new era in pharmaceutics. Besides enabling high-throughput screening with genetic variation, it also is not subjected to safety issues and ethical issues as in human patients.[11]

In cancer research, models have been proposed for the study of cancer pathogenesis and metastasis. A promising field of cancer research that is currently of significant interest is immunotherapy.[11] Antibodies and antibody-recruiting molecules can enhance the immune response against tumours. These molecules can be implemented in 3D bioprinted delivery designs to fight tumours. Another possibility is to adjust a patient's own cytotoxic T cells with chimeric antigen receptors (CARs).[173] CARs are proteins on the T cell surface that recognize a specific protein on the tumour cell membrane. After modification these cytotoxic T cells can be transferred back to the patient, where they can induce apoptosis in tumour cells.

CONCLUSIONS

3D bioprinting has shown great capabilities in the fields of tissue engineering and regenerative medicine, transplantation and clinical applications, drug testing and high-throughput screening, and cancer research. To achieve further progress of 3D bioprinting, advancements must be made at all levels. Bioprinting technologies have to come up with new approaches to cope with the challenges given by current print-heads and nozzles, including printing resolution. New bio-ink materials need to be created to be able to fabricate long-term structural integer complexes with the final goal of creating functional whole human organ complexes. In the future, bioprinting standards need to be implemented to secure progress at each level. 3D bioprinting has made a start in changing healthcare strategies at the level of medical devices, clinical applications, and disease studies. It already has shown its capability in the design of complex architectures in 3D. As a rapidly developing field of research, the capabilities of 3D bioprinting will be expanded further leading to significant advances in science and better healthcare outcomes for patients.

ACKNOWLEDGEMENTS

The authors thank the Monash Warwick Alliance for funding.

ABBREVIATIONS

3D: three-dimensional;

αCD: α-cyclodextrin;

AFS: amniotic fluid-derived;

AM: additive manufacturing

BG: bioactive glass;

BMP-2: bone morphogenetic protein-2;

BMSC: bone marrow stromal cell;

CAR: chimeric antigen receptor;

cmc: critical micelle concentration;

CMC: carboxymethylchitosan;

CNT: carbon nanotube;

CTAB: cetyltrimethylammonium bromide;

dECM: decellularized extracellular matrix;

DBB: droplet-based bioprinting;

DMA: dimethacrylate;

DOD: drop-on-demand;

ECM: extracellular matrix;

ELP: elastin-like peptide;

ELR: elastin-like recombinamer;

EPC: endothelial progenitor cell;

FRESH: freeform reversible embedding of suspended hydrogels;

GelMa: gelatin methacrylate;

GlyEE: glycine ethyl ester;

GNR: gold nanorods;

HA: hyaluronic acid;

HAMA: methacrylated hyaluronic acid;

HepG2: human liver cancer cells;

High Alg: high molecular weight alginate;

hMSCs: human mesenchymal stem cells;

HMVEC: human dermal microvascular endothelial cell;

ICE: ionic-covalent entanglement;

ITOP: integrated tissue-organ printer;

LAP: lithium phenyl-2,4,6-trimethylbenzoylphosphinate;

LCST: lower critical solution temperature;

LIFT: laser-induced forward transfer;

Low Alg: low molecular weight alginate;

MC: methyl cellulose;

MMP: matrix metalloproteinase;

MSC: mesenchymal stem cells;

MW: molecular weight;

NorHA: norbornene-functionalized hyaluronic acid;

PDMS: polydimethylsiloxane;

PEC: polyelectrolyte complex;

PEG: poly(ethylene glycol);

PEGac: acrylate-terminated poly(ethylene glycol);

PEGDA: poly(ethylene glycol) diacrylate;

PEGTA: 4-arm poly(ethylene glycol)-tetra-acrylate;

PCL: poly(ε-caprolactone);

PLGA: poly(D,L-lactic-co-glycolic acid);

PNIPAAM: poly(N-isopropylacrylamide);

PPG: poly(propylene glycol);

RGD: arginine-glycine-aspartic acid;

Sol: colloidal solution.

REFERENCES

1. R. J. Klebe, *Exp. Cell Res.*, 1988, **179**, 362-373.
2. V. Mironov, N. Reis and B. Derby, *Tiss. Eng.*, 2006, **12**, 631-634.
3. S. Vijayavenkataraman, *Artif. Organs*, 2016, **40**, 1033-1038.
4. S. H. Park, C. S. Jung and B. H. Min, *Tiss. Eng. Regen. Med.*, 2016, **13**, 622-635.
5. H. Gudapati, M. Dey and I. Ozbolat, *Biomaterials*, 2016, **102**, 20-42.
6. J. E. Kim, S. H. Kim and Y. Jung, *Tiss. Eng. Regen. Med.*, 2016, **13**, 636-646.
7. V. Mironov, V. Kasyanov and R. R. Markwald, *Curr. Opin. Biotech.*, 2011, **22**, 667-673.
8. N. E. Fedorovich, H. M. Wijnberg, W. J. A. Dhert and J. Alblas, *Tiss. Eng. Pt. A*, 2011, **17**, 2113-2121.
9. L. Koch, A. Deiwick, S. Schlie, S. Michael, M. Gruene, V. Coger, D. Zychlinski, A. Schambach, K. Reimers, P. M. Vogt and B. Chichkov, *Biotechnol. Bioeng.*, 2012, **109**, 1855-1863.
10. V. Lee, G. Singh, J. P. Trasatti, C. Bjornsson, X. W. Xu, T. N. Tran, S. S. Yoo, G. H. Dai and P. Karande, *Tiss. Eng. Pt. C-Meth.*, 2014, **20**, 473-484.
11. W. J. Peng, D. Unutmaz and I. T. Ozbolat, *Trends Biotechnol.*, 2016, **34**, 722-732.
12. I. T. Ozbolat and Y. Yu, *IEEE T. Biomed. Eng.*, 2013, **60**, 691-699.
13. H. Lee and D. W. Cho, *Lab Chip*, 2016, **16**, 2618-2625.
14. N. E. Fedorovich, J. R. Dewijn, A. J. Verbout, J. Alblas and W. J. A. Dhert, *Tiss. Eng. Pt. A*, 2008, **14**, 127-133.
15. A. B. Dababneh and I. T. Ozbolat, *J. Manuf. Sci. Eng.-T. ASME*, 2014, **136**, 061016.
16. M. Hospodiuk, M. Dey, D. Sosnoski and I. T. Ozbolat, *Biotechnol. Adv.*, 2017, **35**, 217-239.
17. T. Jungst, W. Smolan, K. Schacht, T. Scheibel and J. Groll, *Chem. Rev.*, 2016, **116**, 1496-1539.
18. Y. J. Seol, H. W. Kang, S. J. Lee, A. Atala and J. J. Yoo, *Eur. J. Cardio-thorac.*, 2014, **46**, 342-348.
19. T. Xu, W. X. Zhao, J. M. Zhu, M. Z. Albanna, J. J. Yoo and A. Atala, *Biomaterials*, 2013, **34**, 130-139.
20. X. F. Cui, K. Breitenkamp, M. G. Finn, M. Lotz and D. D. D'Lima, *Tiss. Eng. Pt. A*, 2012, **18**, 1304-1312.
21. W. Lee, J. C. Debasitis, V. K. Lee, J. H. Lee, K. Fischer, K. Edminster, J. K. Park and S. S. Yoo, *Biomaterials*, 2009, **30**, 1587-1595.
22. A. Faulkner-Jones, C. Fyfe, D. J. Cornelissen, J. Gardner, J. King, A. Courtney and W. M. Shu, *Biofabrication*, 2015, **7**, 044102.
23. U. A. Gurkan, R. El Assal, S. E. Yildiz, Y. Sung, A. J. Trachtenberg, W. P. Kuo and U. Demirci, *Mol. Pharm.*, 2014, **11**, 2151-2159.

24. Z. L. Yue, X. Liu, P. T. Coates and G. G. Wallace, *Curr. Opin. Organ. Tran.*, 2016, **21**, 467-475.
25. C. M. Owens, F. Marga, G. Forgacs and C. M. Heesch, *Biofabrication*, 2013, **5**, 045007.
26. V. Mironov, R. P. Visconti, V. Kasyanov, G. Forgacs, C. J. Drake and R. R. Markwald, *Biomaterials*, 2009, **30**, 2164-2174.
27. A. N. Mehesz, J. Brown, Z. Hajdu, W. Beaver, J. V. L. da Silva, R. P. Visconti, R. R. Markwald and V. Mironov, *Biofabrication*, 2011, **3**, 025002.
28. I. T. Ozbolat, *Trends Biotechnol.*, 2015, **33**, 395-400.
29. I. T. Ozbolat, H. Chen and Y. Yu, *Robot. Cim.-Int. Manuf.*, 2014, **30**, 295-304.
30. K. Markstedt, A. Mantas, I. Tournier, H. M. Avila, D. Hagg and P. Gatenholm, *Biomacromolecules*, 2015, **16**, 1489-1496.
31. M. Kesti, C. Eberhardt, G. Pagliccia, D. Kenkel, D. Grande, A. Boss and M. Zenobi-Wong, *Adv. Funct. Mater.*, 2015, **25**, 7406-7417.
32. B. Duan, L. A. Hockaday, K. H. Kang and J. T. Butcher, *J. Biomed. Mater. Res. A*, 2013, **101**, 1255-1264.
33. B. Duan, E. Kapetanovic, L. A. Hockaday and J. T. Butcher, *Acta Biomater.*, 2014, **10**, 1836-1846.
34. R. Lozano, L. Stevens, B. C. Thompson, K. J. Gilmore, R. Gorkin, E. M. Stewart, M. I. H. Panhuis, M. Romero-Ortega and G. G. Wallace, *Biomaterials*, 2015, **67**, 264-273.
35. W. J. Liu, Y. S. Zhang, M. A. Heinrich, F. De Ferrari, H. L. Jang, S. M. Bakht, M. M. Alvarez, J. Z. Yang, Y. C. Li, G. Trujillo-de Santiago, A. K. Miri, K. Zhu, P. Khoshakhlagh, G. Prakash, H. Cheng, X. F. Guan, Z. Zhong, J. Ju, G. H. Zhu, X. Y. Jin, S. R. Shin, M. R. Dokmeci and A. Khademhosseini, *Adv. Mater.*, 2017, **29**, 1604630.
36. D. J. Odde and M. J. Renn, *Trends Biotechnol.*, 1999, **17**, 385-389.
37. J. A. Barron, B. R. Ringeisen, H. S. Kim, B. J. Spargo and D. B. Chrisey, *Thin Solid Film.*, 2004, **453**, 383-387.
38. C. Mandrycky, Z. J. Wang, K. Kim and D. H. Kim, *Biotechnol. Adv.*, 2016, **34**, 422-434.
39. L. Koch, S. Kuhn, H. Sorg, M. Gruene, S. Schlie, R. Gaebel, B. Polchow, K. Reimers, S. Stoelting, N. Ma, P. M. Vogt, G. Steinhoff and B. Chichkov, *Tiss. Eng. Pt. C-Meth.*, 2010, **16**, 847-854.
40. F. Pati, J. Jang, D. H. Ha, S. W. Kim, J. W. Rhie, J. H. Shim, D. H. Kim and D. W. Cho, *Nat. Commun.*, 2014, **5**, 3935.
41. H. W. Kang, S. J. Lee, I. K. Ko, C. Kengla, J. J. Yoo and A. Atala, *Nat. Biotechnol.*, 2016, **34**, 312-319.
42. J. M. Lee and W. Y. Yeong, *Adv. Healthc. Mater*, 2016, **5**, 2856-2865.
43. I. T. Ozbolat and M. Hospodiuk, *Biomaterials*, 2016, **76**, 321-343.
44. S. Kashte, A. K. Jaiswal and S. Kadam, *Tiss. Eng. Regen. Med.*, 2017, **14**, 1-14.
45. Y. Yu, K. K. Moncal, J. Q. Li, W. J. Peng, I. Rivero, J. A. Martin and I. T. Ozbolat, *Sci. Rep.*, 2016, **6**, 28714.
46. A. C. Daly, G. M. Cunniffe, B. N. Sathy, O. Jeon, E. Alsberg and D. J. Kelly, *Adv. Healthc. Mater*, 2016, **5**, 2353-2362.
47. H. P. Tan and K. G. Marra, *Materials*, 2010, **3**, 1746-1767.
48. G. D. Nicodemus and S. J. Bryant, *Tiss. Eng. Pt. B-Rev.*, 2008, **14**, 149-165.
49. A. Munaz, R. K. Vadivelu, J. S. John, M. Barton, H. Kamble and N.-T. Nguyen, *J. Sci. Adv. Mater. Dev.*, 2016, **1**, 1-17.
50. T. Billiet, M. Vandenhaute, J. Schelfhout, S. Van Vlierberghe and P. Dubruel, *Biomaterials*, 2012, **33**, 6020-6041.

51. J. Malda, J. Visser, F. P. Melchels, T. Jungst, W. E. Hennink, W. J. A. Dhert, J. Groll and D. W. Hutmacher, *Adv. Mater.*, 2013, **25**, 5011-5028.
52. M. Maeda, S. Tani, A. Sano and K. Fujioka, *J. Control. Rel.*, 1999, **62**, 313-324.
53. R. Suntornnond, J. An and C. K. Chua, *Macromol. Mater. Eng.*, 2017, **302**, 1600266.
54. M. R. Matanovic, J. Kristl and P. A. Grabnar, *Int. J. Pharm.*, 2014, **472**, 262-275.
55. F. P. W. Melchels, M. A. N. Domingos, T. J. Klein, J. Malda, P. J. Bartolo and D. W. Hutmacher, *Prog. Polym. Sci.*, 2012, **37**, 1079-1104.
56. D. B. Kolesky, R. L. Truby, A. S. Gladman, T. A. Busbee, K. A. Homan and J. A. Lewis, *Adv. Mater.*, 2014, **26**, 3124-3130.
57. E. Hoch, T. Hirth, G. E. M. Tovar and K. Borchers, *J. Mater. Chem. B*, 2013, **1**, 5675-5685.
58. A. Ovsianikov, S. Muhleder, J. Torgersen, Z. Q. Li, X. H. Qin, S. Van Vlierberghe, P. Dubruel, W. Holnthoner, H. Redl, R. Liska and J. Stampfl, *Langmuir*, 2014, **30**, 3787-3794.
59. Y. S. Zhang, A. Arneri, S. Bersini, S. R. Shin, K. Zhu, Z. Goli-Malekabadi, J. Aleman, C. Colosi, F. Busignani, V. Dell'Erba, C. Bishop, T. Shupe, D. Demarchi, M. Moretti, M. Rasponi, M. R. Dokmeci, A. Atala and A. Khademhosseini, *Biomaterials*, 2016, **110**, 45-59.
60. T. Billiet, E. Gevaert, T. De Schryver, M. Cornelissen and P. Dubruel, *Biomaterials*, 2014, **35**, 49-62.
61. J. W. Nichol, S. T. Koshy, H. Bae, C. M. Hwang, S. Yamanlar and A. Khademhosseini, *Biomaterials*, 2010, **31**, 5536-5544.
62. Y. Chau, Y. Luo, A. C. Y. Cheung, Y. Nagai, S. G. Zhang, J. B. Kobler, S. M. Zeitels and R. Langer, *Biomaterials*, 2008, **29**, 1713-1719.
63. A. Skardal, J. X. Zhang, L. McCoard, X. Y. Xu, S. Oottamasathien and G. D. Prestwich, *Tiss. Eng. Pt. A*, 2010, **16**, 2675-2685.
64. T. J. Hinton, Q. Jallerat, R. N. Palchesko, J. H. Park, M. S. Grodzicki, H.-J. Shue, M. H. Ramadan, A. R. Hudson and A. W. Feinberg, *Sci. Adv.*, 2015, **1**, e1500758.
65. B. H. Lee, N. Lum, L. Y. Seow, P. Q. Lim and L. P. Tan, *Materials*, 2016, **9**, 797.
66. W. T. Jia, P. S. Gungor-Ozkerim, Y. S. Zhang, K. Yue, K. Zhu, W. J. Liu, Q. Pi, B. Byambaa, M. R. Dokmeci, S. R. Shin and A. Khademhosseini, *Biomaterials*, 2016, **106**, 58-68.
67. K. Zhu, S. R. Shin, T. van Kempen, Y. C. Li, V. Ponraj, A. Nasajpour, S. Mandla, N. Hu, X. Liu, J. Leijten, Y. D. Lin, M. A. Hussain, Y. S. Zhang, A. Tamayol and A. Khademhosseini, *Adv. Funct. Mater.*, 2017, **27**, 1605352.
68. M. D. Shoulders and R. T. Raines, in *Annual Review of Biochemistry*, 2009, vol. 78, pp. 929-958.
69. J. H. Lee, A. El-Fiqi, C. M. Han and H. W. Kim, *Tiss. Eng. Regen. Med.*, 2015, **12**, 90-97.
70. A. Skardal, D. Mack, E. Kapetanovic, A. Atala, J. D. Jackson, J. Yoo and S. Soker, *Stem Cell. Transl. Med.*, 2012, **1**, 792-802.
71. S. Rhee, J. L. Puetzer, B. N. Mason, C. A. Reinhart-King and L. J. Bonassar, *ACS Biomater. Sci. Eng.*, 2016, **2**, 1800-1805.
72. Y. B. Kim, H. J. Lee and G. H. Kim, *ACS Appl. Mater. Interf.*, 2016, **8**, 32230-32240.
73. S. Chattopadhyay and R. T. Raines, *Biopolymers*, 2014, **101**, 821-833.
74. J. Y. Park, J. C. Choi, J. H. Shim, J. S. Lee, H. Park, S. W. Kim, J. Doh and D. W. Cho, *Biofabrication*, 2014, **6**, 035004.
75. J. H. Shim, K. M. Jang, S. K. Hahn, J. Y. Park, H. Jung, K. Oh, K. M. Park, J. Yeom, S. H. Park, S. W. Kim, J. H. Wang, K. Kim and D. W. Cho, *Biofabrication*, 2016, **8**, 014102.
76. J. W. Lee, Y. J. Choi, W. J. Yong, F. Pati, J. H. Shim, K. S. Kang, I. H. Kang, J. Park and D. W. Cho, *Biofabrication*, 2016, **8**, 015007.
77. L. Gasperini, J. F. Mano and R. L. Reis, *J. Roy. Soc. Interf.*, 2014, **11**, 20140817.

78. S. G. Wise and A. S. Weiss, *Int. J. Biochem. Cell Biol.*, 2009, **41**, 494-497.
79. J. C. Rodriguez-Cabello, L. Martin, M. Alonso, F. J. Arias and A. M. Testera, *Polymer*, 2009, **50**, 5159-5169.
80. E. Servoli, D. Maniglio, A. Motta and C. Migliaresi, *Macromol. Biosci.*, 2008, **8**, 827-835.
81. G. M. Nogueira, M. A. de Moraes, A. C. D. Rodas, O. Z. Higa and M. M. Beppu, *Mater. Sci. Eng. C-Mater.*, 2011, **31**, 997-1001.
82. U. J. Kim, J. Y. Park, C. M. Li, H. J. Jin, R. Valluzzi and D. L. Kaplan, *Biomacromolecules*, 2004, **5**, 786-792.
83. Y. Qi, H. Wang, K. Wei, Y. Yang, R. Y. Zheng, I. S. Kim and K. Q. Zhang, *Int. J. Mol. Sci.*, 2017, **18**, 237.
84. S. Das, F. Pati, Y. J. Choi, G. Rijal, J. H. Shim, S. W. Kim, A. R. Ray, D. W. Cho and S. Ghosh, *Acta Biomater.*, 2015, **11**, 233-246.
85. M. J. Rodriguez, J. Brown, J. Giordano, S. J. Lin, F. G. Omenetto and D. L. Kaplan, *Biomaterials*, 2017, **117**, 105-115.
86. P. A. Janmey, J. P. Winer and J. W. Weisel, *J. Roy. Soc. Interf.*, 2009, **6**, 1-10.
87. X. F. Cui and T. Boland, *Biomaterials*, 2009, **30**, 6221-6227.
88. T. Xu, C. A. Gregory, P. Molnar, X. Cui, S. Jalota, S. B. Bhaduri and T. Boland, *Biomaterials*, 2006, **27**, 3580-3588.
89. K. L. Zhang, Q. Fu, J. Yoo, X. X. Chen, P. Chandra, X. M. Mo, L. J. Song, A. Atala and W. X. Zhao, *Acta Biomater.*, 2017, **50**, 154-164.
90. K. Y. Lee and D. J. Mooney, *Prog. Polym. Sci.*, 2012, **37**, 106-126.
91. J. Munguia-Lopez, T. Jiang, E. Munoz-Sandoval, A. De Leon-Rodriguez and J. Kinsella, *Tiss. Eng. Pt. A*, 2016, **22**, S145-S145.
92. A. L. Torres, V. M. Gaspar, I. R. Serra, G. S. Diogo, R. Fradique, A. P. Silva and I. J. Correia, *Mater. Sci. Eng. C-Mater.*, 2013, **33**, 4460-4469.
93. J. Park, S. J. Lee, S. Chung, J. H. Lee, W. D. Kim, J. Y. Lee and S. A. Park, *Mater. Sci. Eng. C-Mater.*, 2017, **71**, 678-684.
94. R. T. Xiong, Z. Y. Zhang, W. X. Chai, D. B. Chrisey and Y. Huang, *Biofabrication*, 2017, **9**.
95. W. Y. J. Chen and G. Abatangelo, *Wound Repair Regen.*, 1999, **7**, 79-89.
96. Y. Yeo, C. B. Highley, E. Bellas, T. Ito, R. Marini, R. Langer and D. S. Kohane, *Biomaterials*, 2006, **27**, 4698-4705.
97. M. N. Collins and C. Birkinshaw, *J. Appl. Polym. Sci.*, 2007, **104**, 3183-3191.
98. L. L. Ouyang, C. B. Highley, C. B. Rodell, W. Sun and J. A. Burdick, *ACS Biomater. Sci. Eng.*, 2016, **2**, 1743-1751.
99. M. T. Poldervaart, B. Goversen, M. de Ruijter, A. Abbadessa, F. P. W. Melchels, F. C. Oner, W. J. A. Dhert, T. Vermonden and J. Alblas, *PLoS One*, 2017, **12**.
100. L. E. Bertassoni, M. Cecconi, V. Manoharan, M. Nikkhah, J. Hjortnaes, A. L. Cristino, G. Barabaschi, D. Demarchi, M. R. Dokmeci, Y. Z. Yang and A. Khademhosseini, *Lab Chip*, 2014, **14**, 2202-2211.
101. Y. J. Tan, X. P. Tan, W. Y. Yeong and S. B. Tor, *Sci. Rep.*, 2016, **6**, 39140.
102. A. C. Daly, S. E. Critchley, E. M. Rencsok and D. J. Kelly, *Biofabrication*, 2016, **8**.
103. Q. Gu, E. Tomaskovic-Crook, R. Lozano, Y. Chen, R. M. Kapsa, Q. Zhou, G. G. Wallace and J. M. Crook, *Adv. Healthc. Mater*, 2016, **5**, 1429-1438.
104. K. S. Hossain, K. Miyanaga, H. Maeda and N. Nemoto, *Biomacromolecules*, 2001, **2**, 442-449.
105. V. L. Campo, D. F. Kawano, D. B. da Silva and I. Carvalho, *Carbohyd. Polym.*, 2009, **77**, 167-180.

106. A. S. Michel, M. M. Mestdagh and M. A. V. Axelos, *Int. J. Biol. Macromol.*, 1997, **21**, 195-200.
107. S. E. Bakarich, P. Balding, R. Gorkin, G. M. Spinks and M. I. H. Panhuis, *RSC Adv.*, 2014, **4**, 38088-38092.
108. P. L. Nasatto, F. Pignon, J. L. M. Silveira, M. E. R. Duarte, M. D. Noseda and M. Rinaudo, *Polymers*, 2015, **7**, 777-803.
109. P. E. Jansson, B. Lindberg and P. A. Sandford, *Carbohyd. Res.*, 1983, **124**, 135-139.
110. J. T. Oliveira, L. Martins, R. Picciochi, I. B. Malafaya, R. A. Sousa, N. M. Neves, J. F. Mano and R. L. Reis, *J. Biomed. Mater. Res. A*, 2010, **93A**, 852-863.
111. J. Silva-Correia, J. M. Oliveira, S. G. Caridade, J. T. Oliveira, R. A. Sousa, J. F. Mano and R. L. Reis, *J. Tissue Eng. Regen. Med.*, 2011, **5**, E97-E107.
112. M. Muller, E. Ozturk, O. Arlov, P. Gatenholm and M. Zenobi-Wong, *Ann. Biomed. Eng.*, 2017, **45**, 210-223.
113. M. Muller, J. Becher, M. Schnabelrauch and M. Zenobi-Wong, *Biofabrication*, 2015, **7**, 035006.
114. M. Muller, J. Becher, M. Schnabelrauch and M. Zenobi-Wong, *J. Vis. Exp.*, 2013, e50632.
115. E. Gioffredi, M. Boffito, S. Calzone, S. M. Giannitelli, A. Rainer, M. Trombetta, P. Mozetic and V. Chiono, in *Second CIRP Conference on Biomanufacturing*, 2016, vol. 49, pp. 125-132.
116. R. Suntornnond, E. Y. S. Tan, J. An and C. K. Chua, *Materials*, 2016, **9**, 756.
117. S. M. Hong, D. Sycks, H. F. Chan, S. T. Lin, G. P. Lopez, F. Guilak, K. W. Leong and X. H. Zhao, *Adv. Mater.*, 2015, **27**, 4035-4040.
118. R. Censi, W. Schuurman, J. Malda, G. di Dato, P. E. Burgisser, W. J. A. Dhert, C. F. van Nostrum, P. di Martino, T. Vermonden and W. E. Hennink, *Adv. Funct. Mater.*, 2011, **21**, 1833-1842.
119. T.-C. Tseng, F.-Y. Hsieh, P. Theato, Y. Wei and S.-H. Hsu, *Biomaterials*, 2017, **133**, 20-28.
120. L. Klouda, *Eur. J. Pharm. Biopharm.*, 2015, **97**, 338-349.
121. H. R. Allcock and R. L. Kugel, *J. Am. Chem. Soc.*, 1965, **87**, 4216-&.
122. J. I. Kim, C. Chun, B. Kim, J. M. Hong, J. K. Cho, S. H. Lee and S. C. Song, *Biomaterials*, 2012, **33**, 218-224.
123. C. Chun, H. J. Lim, K. Y. Hong, K. H. Park and S. C. Song, *Biomaterials*, 2009, **30**, 6295-6308.
124. M. R. Park, C. Chun, C. S. Cho and S. C. Song, *Eur. J. Pharm. Biopharm.*, 2010, **76**, 179-188.
125. M. R. Park, B. B. Seo and S. C. Song, *Biomaterials*, 2013, **34**, 1327-1336.
126. Z. J. Huang, X. W. Liu, S. S. Chen, Q. H. Lu and G. Sun, *Polym. Chem.*, 2015, **6**, 143-149.
127. R. F. Pereira and P. J. Bartolo, *J. Appl. Polym. Sci.*, 2015, **132**, 42458.
128. L. L. Ouyang, C. B. Highley, W. Sun and J. A. Burdick, *Adv. Mater.*, 2017, **29**, 1604983.
129. R. Levato, J. Visser, J. A. Planell, E. Engel, J. Malda and M. A. Mateos-Timoneda, *Biofabrication*, 2014, **6**, 035020.
130. J. Malda and C. G. Frondoza, *Trends Biotechnol.*, 2006, **24**, 299-304.
131. P. H. Jakob, J. Kehrer, P. Flood, C. Wiegel, U. Haselmann, M. Meissner, E. H. K. Stelzer and E. G. Reynaud, *Cytotechnology*, 2016, **68**, 1813-1825.
132. A. V. Goncharenko, N. V. Malyuchenko, A. M. Moisenovich, M. S. Kotlyarova, A. Y. Arkhipova, A. S. Kon'kov, Agapov, II, A. V. Molochkov, M. M. Moisenovich and M. P. Kirpichnikov, *Dokl. Biochem. Biophys.*, 2016, **470**, 368-370.
133. S. M. Albelda and C. A. Buck, *FASEB J.*, 1990, **4**, 2868-2880.
134. S. V. Murphy and A. Atala, *Nat. Biotechnol.*, 2014, **32**, 773-785.
135. A. Akkouch, Y. Yu and I. T. Ozbolat, *Biofabrication*, 2015, **7**, 031002.
136. D. Del Duca, T. Werbowetski and R. F. Del Maestro, *J Neurooncol*, 2004, **67**, 295-303.

137. F. Guo, P. Li, J. B. French, Z. M. Mao, H. Zhao, S. X. Li, N. Nama, J. R. Fick, S. J. Benkovic and T. J. Huang, *Proc. Natl. Acad. Sci. USA*, 2015, **112**, 43-48.
138. W. Metzger, S. Rother, T. Pohlemann, S. Moller, M. Schnabelrauch, V. Hintze and D. Scharnweber, *Mater. Sci. Eng. C-Mater.*, 2017, **73**, 310-318.
139. H. Tseng, J. A. Gage, T. W. Shen, W. L. Haisler, S. K. Neeley, S. Shiao, J. B. Chen, P. K. Desai, A. Liao, C. Hebel, R. M. Raphael, J. L. Becker and G. R. Souza, *Sci. Rep.*, 2015, **5**, 13987.
140. C. Kucukgul, S. B. Ozler, I. Inci, E. Karakas, S. Irmak, D. Gozuacik, A. Taralp and B. Koc, *Biotechnol. Bioeng.*, 2015, **112**, 811-821.
141. K. Schrobback, T. J. Klein, R. Crawford, Z. Upton, J. Malda and D. I. Leavesley, *Cell Tissue Res.*, 2012, **347**, 649-663.
142. F. Pati, D. H. Ha, J. Jang, H. H. Han, J. W. Rhie and D. W. Cho, *Biomaterials*, 2015, **62**, 164-175.
143. S. Schwarz, L. Koerber, A. F. Elsaesser, E. Goldberg-Bockhorn, A. M. Seitz, L. Durselen, A. Ignatius, P. Walther, R. Breiter and N. Rotter, *Tiss. Eng. Pt. A*, 2012, **18**, 2195-2209.
144. H. C. Ott, T. S. Matthiesen, S. K. Goh, L. D. Black, S. M. Kren, T. I. Netoff and D. A. Taylor, *Nat. Med.*, 2008, **14**, 213-221.
145. P. M. Crapo, T. W. Gilbert and S. F. Badylak, *Biomaterials*, 2011, **32**, 3233-3243.
146. S. Singh, I. O. Afara, A. H. Tehrani and A. Oloyede, *Tiss. Eng. Regen. Med.*, 2015, **12**, 294-305.
147. J. Jang, T. G. Kim, B. S. Kim, S. W. Kim, S. M. Kwon and D. W. Cho, *Acta Biomater.*, 2016, **33**, 88-95.
148. J. R. Xavier, T. Thakur, P. Desai, M. K. Jaiswal, N. Sears, E. Cosgriff-Hernandez, R. Kaunas and A. K. Gaharwar, *ACS Nano*, 2015, **9**, 3109-3118.
149. G. F. Gao, A. F. Schilling, T. Yonezawa, J. Wang, G. H. Dai and X. F. Cui, *Biotechnol. J.*, 2014, **9**, 1304-1311.
150. W. Lee, J. Pinckney, V. Lee, J. H. Lee, K. Fischer, S. Polio, J. K. Park and S. S. Yoo, *Neuroreport*, 2009, **20**, 798-803.
151. Y. B. Lee, S. Polio, W. Lee, G. H. Dai, L. Menon, R. S. Carroll and S. S. Yoo, *Exp. Neurol.*, 2010, **223**, 645-652.
152. D. A. Zopf, S. J. Hollister, M. E. Nelson, R. G. Ohye and G. E. Green, *New Engl. J. Med.*, 2013, **368**, 2043-2045.
153. G. M. Cooper, E. D. Miller, G. E. DeCesare, A. Usas, E. L. Lensie, M. R. Bykowski, J. Huard, L. E. Weiss, J. E. Losee and P. G. Campbell, *Tiss. Eng. Pt. A*, 2010, **16**, 1749-1759.
154. T. P. Richardson, M. C. Peters, A. B. Ennett and D. J. Mooney, *Nat. Biotechnol.*, 2001, **19**, 1029-1034.
155. H. Jeon, K. Kang, S. A. Park, W. D. Kim, S. S. Paik, S. H. Lee, J. Jeong and D. Choi, *Gut Liver*, 2017, **11**, 121-128.
156. 3D Printing of Medical Devices, http://www.fda.gov/MedicalDevices/ProductsandMedicalProcedures/3DPrintingofMedicalDevices/, (accessed 04/05/2017).
157. N. Cubo, M. Garcia, J. F. del Canizo, D. Velasco and J. L. Jorcano, *Biofabrication*, 2017, **9**, 015006.
158. J. A. DiMasi, H. G. Grabowski and R. W. Hansen, *New Engl. J. Med.*, 2015, **372**, 1972-1972.
159. M. J. Waring, J. Arrowsmith, A. R. Leach, P. D. Leeson, S. Mandrell, R. M. Owen, G. Pairaudeau, W. D. Pennie, S. D. Pickett, J. B. Wang, O. Wallace and A. Weir, *Nat. Rev. Drug Discov.*, 2015, **14**, 475-486.

160. M. Rimann and U. Graf-Hausner, *Curr. Opin. Biotech.*, 2012, **23**, 803-809.
161. A. K. Gaharwar, A. Arpanaei, T. L. Andresen and A. Dolatshahi-Pirouz, *Adv. Mater.*, 2016, **28**, 771-781.
162. X. K. Li, X. Y. Zhang, S. Zhao, J. Y. Wang, G. Liu and Y. N. Du, *Lab Chip*, 2014, **14**, 471-481.
163. M. Centola, F. Abbruzzese, C. Scotti, A. Barbero, G. Vadala, V. Denaro, I. Martin, M. Trombetta, A. Rainer and A. Marsano, *Tiss. Eng. Pt. A*, 2013, **19**, 1960-1971.
164. F. Xu, J. Celli, I. Rizvi, S. Moon, T. Hasan and U. Demirci, *Biotechnol. J.*, 2011, **6**, 204-212.
165. X. Zhou, W. Zhu, M. Nowicki, S. Miao, H. T. Cui, B. Holmes, R. I. Glazer and L. G. Zhang, *ACS Appl. Mater. Interf.*, 2016, **8**, 30017-30026.
166. Y. Yu, Y. H. Zhang and I. T. Ozbolat, *J. Manuf. Sci. Eng.-T. ASME*, 2014, **136**.
167. D. B. Kolesky, K. A. Homan, M. A. Skylar-Scott and J. A. Lewis, *Proc. Natl. Acad. Sci. USA*, 2016, **113**, 3179-3184.
168. E. Bianconi, A. Piovesan, F. Facchin, A. Beraudi, R. Casadei, F. Frabetti, L. Vitale, M. C. Pelleri, S. Tassani, F. Piva, S. Perez-Amodio, P. Strippoli and S. Canaider, *Ann. Hum. Biol.*, 2013, **40**, 463-471.
169. A. V. Do, B. Khorsand, S. M. Geary and A. K. Salem, *Adv. Healthc. Mater*, 2015, **4**, 1742-1762.
170. A. J. Engler, S. Sen, H. L. Sweeney and D. E. Discher, *Cell*, 2006, **126**, 677-689.
171. V. K. Lee, A. M. Lanzi, H. Ngo, S. S. Yoo, P. A. Vincent and G. H. Dai, *Cell Mol. Bioeng.*, 2014, **7**, 460-472.
172. B. Gao, Q. Z. Yang, X. Zhao, G. R. Jin, Y. F. Ma and F. Xu, *Trends Biotechnol.*, 2016, **34**, 746-756.
173. D. N. Khalil, E. L. Smith, R. J. Brentjens and J. D. Wolchok, *Nat. Rev. Clin. Oncol.*, 2016, **13**, 273-290.
174. A. Thakur, M. K. Jaiswal, C. W. Peak, J. K. Carrow, J. Gentry, A. Dolatshahi-Pirouz and A. K. Gaharwar, *Nanoscale*, 2016, **8**, 12362-12372.
175. M. K. Wlodarczyk-Biegun and A. del Campo, *Biomaterials*, 2017, **134**, 180-201.
176. V. H. M. Mouser, F. P. W. Melchels, J. Visser, W. J. A. Dhert, D. Gawlitta and J. Malda, *Biofabrication*, 2016, **8**.
177. S. Scaglione, R. Barenghi, S. Beke, L. Ceseracciu, I. Romano, F. Sbrana, P. Stagnaro, F. Brandi and M. Vassalli, in *Optical Methods for Inspection, Characterization, and Imaging of Biomaterials*, Spie-Int Soc Optical Engineering, Bellingham, 2013, vol. 8792.
178. M. R. Sommer, M. Schaffner, D. Carnelli and A. R. Studart, *ACS Appl. Mater. Interf.*, 2016, **8**, 34677-34685.
179. R. Suntivich, I. Drachuk, R. Calabrese, D. L. Kaplan and V. V. Tsukruk, *Biomacromolecules*, 2014, **15**, 1428-1435.
180. B. Guillotin, A. Souquet, S. Catros, M. Duocastella, B. Pippenger, S. Bellance, R. Bareille, M. Remy, L. Bordenave, J. Amedee and F. Guillemot, *Biomaterials*, 2010, **31**, 7250-7256.

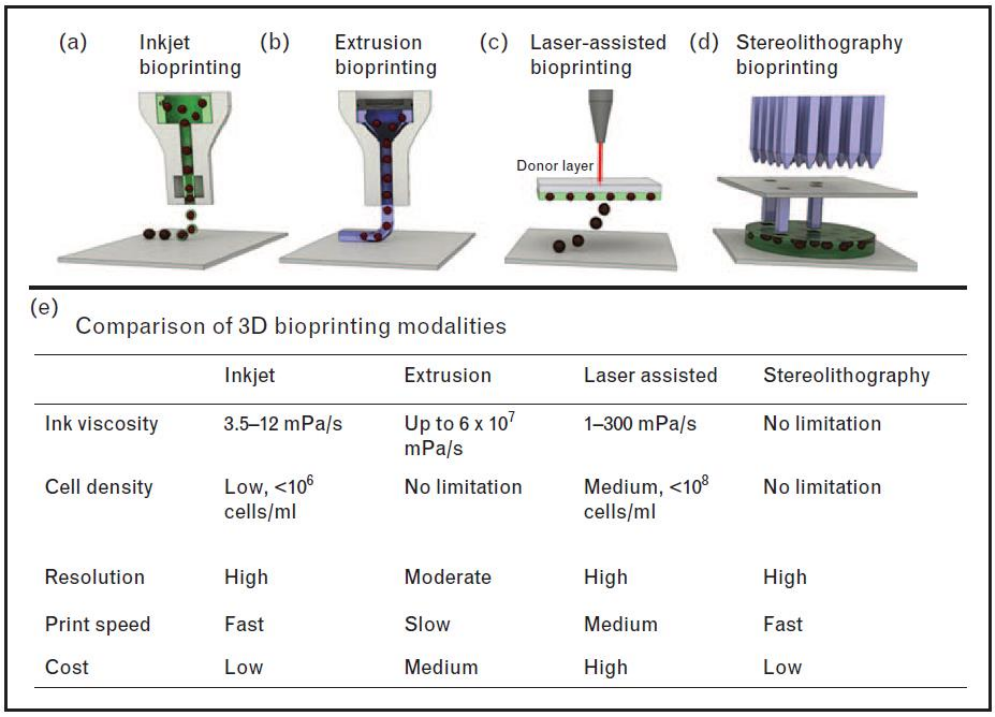

(e) Comparison of 3D bioprinting modalities

	Inkjet	Extrusion	Laser assisted	Stereolithography
Ink viscosity	3.5–12 mPa/s	Up to 6 x 10^7 mPa/s	1–300 mPa/s	No limitation
Cell density	Low, $<10^6$ cells/ml	No limitation	Medium, $<10^8$ cells/ml	No limitation
Resolution	High	Moderate	High	High
Print speed	Fast	Slow	Medium	Fast
Cost	Low	Medium	High	Low

Figure 1. Schematic representation of bioprinting technologies. (a) inkjet bioprinting includes continuous, drop-on-demand, and electrohydrodynamic jetting. (b) Extrusion-based printing. (c) Laser-assisted (also known as laser-induced forward transfer) bioprinting. (d) Stereolithography. (e) Comparison of the techniques a-d. Figure reproduced with permission from [24], © Wolters Kluwer Health, Inc., 2016.

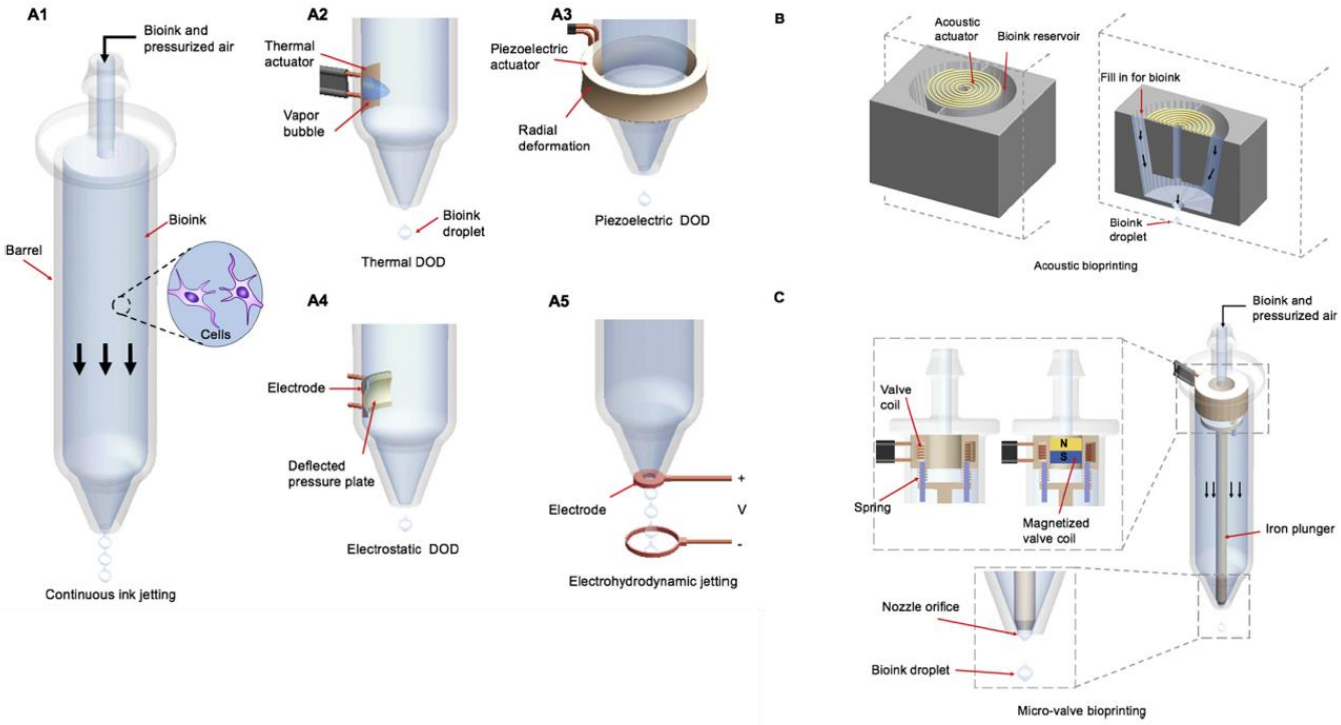

Figure 2. Droplet-based bioprinting. A1) Continuous ink jetting, A2) Thermal drop-on-demand inkjet bioprinting, A3) Piezoelectric drop-on-demand inkjet bioprinting, A4) Electrostatic drop-on-demand inkjet bioprinting, A5) Electrohydrodynamic jet bioprinting; B) Acoustic-droplet-ejection bioprinting; C) Micro-valve bioprinting. Reproduced with permission from [5], © Elsevier, 2016.

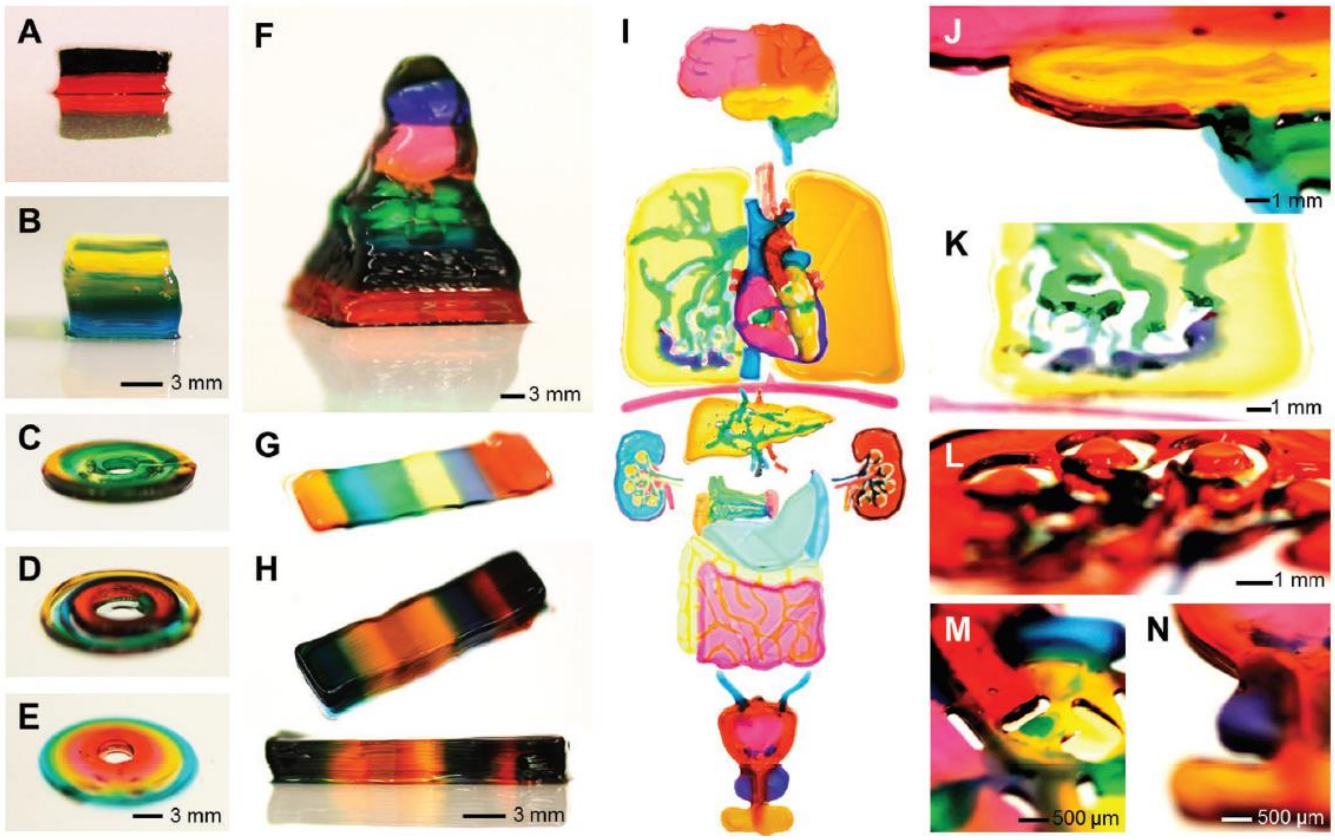

Figure 3. 3D bioprinted constructs by rapid continuous multimaterial extrusion bioprinting. A) Dual-layered cuboid block, B) triple-layered cuboid block, C-E) blood-vessel like constructs of dual, triple, and quadruple materials, respectively, F) seven material-containing pyramid, G-H) continuous segments of seven different bio-inks in three- and ten-layered blocks, I) separately printed organ-like constructs from multiple bio-inks, stitched together for photograph, J-N) side views of constructs in 'I)' to show 3D nature; J) brain, K) lung vascular, L) kidney, M) left atrium (heart), N) bladder/prostate. Reproduced with permission from [35], © John Wiley & Sons, 2016.

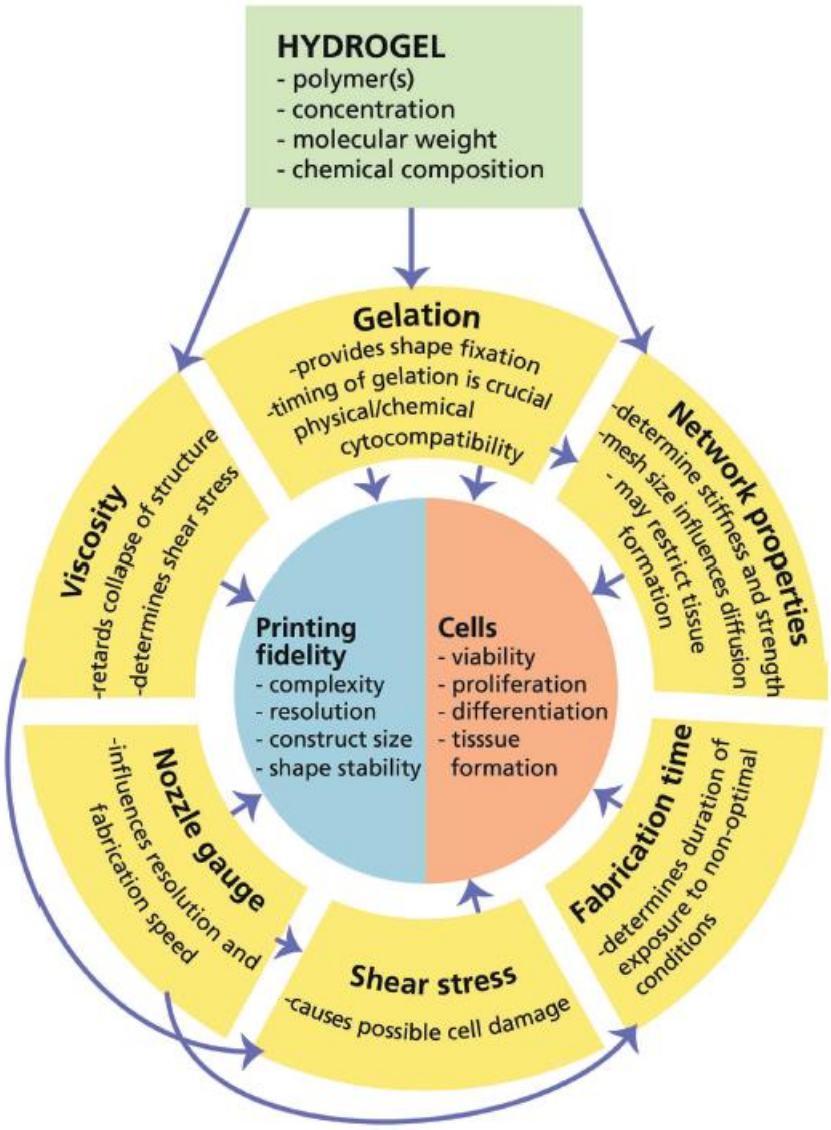

Figure 4. Summary of influential factors on printing fidelity and cells, and their relations critical to biofabrication. Reproduced with permission from [51], © John Wiley & Sons, 2013.

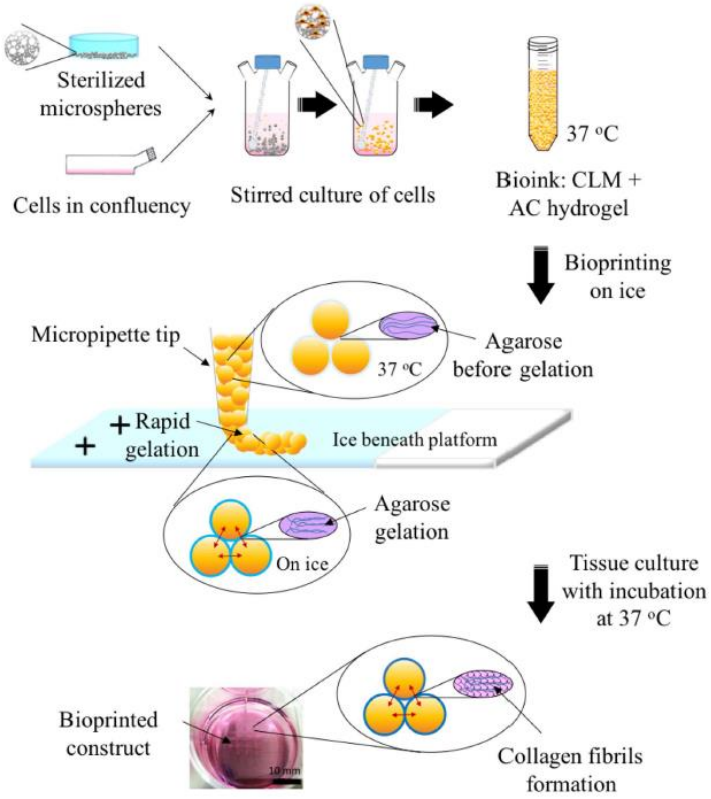

Figure 5. Schematic illustration of the fabrication of PLGA porous microspheres containing mouse fibroblasts in an agarose-collagen hydrogel. Mouse fibroblasts (in orange) are seeded on the microspheres. Stirred culturing allows infiltration and proliferation of the cells in the microspheres, creating cell-laden microspheres (CLMs). The CLMs are then encapsulated in the agarose-collagen hydrogel. This hydrogel undergoes gelation after printing on the chilled platform. Collagen fibrils form on culturing at 37°C. Reproduced from [101] under a Creative Commons CC-BY licence (authors: Y. J. Tan, X. P. Tan, W. Y. Yeong and S. B. Tor).

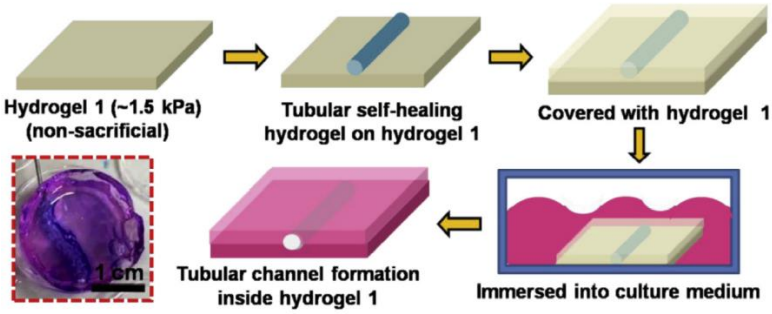

Figure 6. Fabrication of a vascularized construct using a glucose-sensitive self-healing hydrogel and a non-glucose sensitive cell-laden hydrogel. Culture medium dissolves glucose-sensitive hydrogel leading to tubular channels in non-glucose sensitive gel. Reproduced with permission from [119], © Elsevier, 2017.

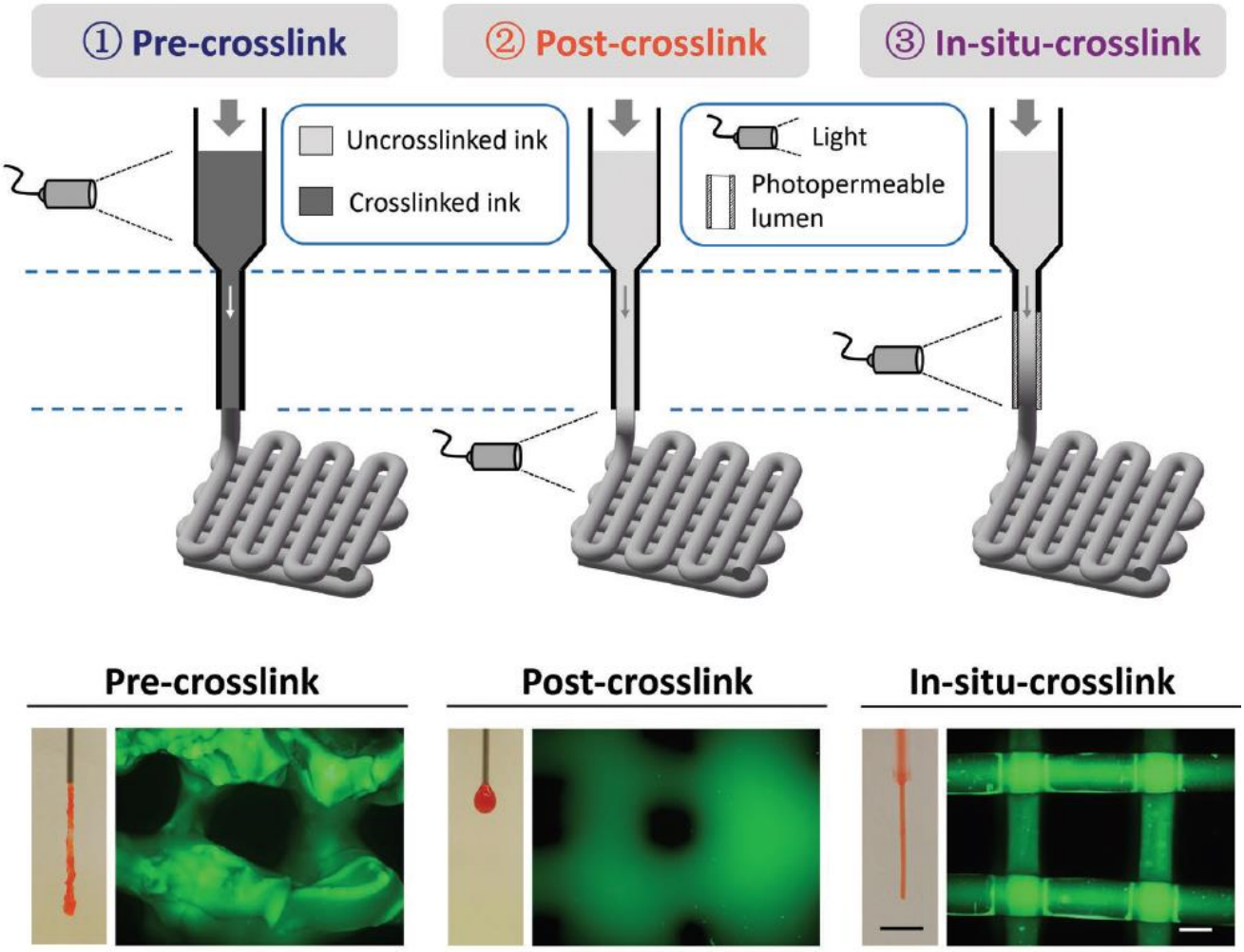

Figure 7. Comparison of the "in-situ-bioprinting" approach to pre- and post-crosslinking approaches. Figure presents schematic representations of each approach (above) and nozzle deposition with the associated printed lattice structure (below). Reproduced with permission from [128], © John Wiley & Sons, 2016.

Table 1. Bio-ink material characteristics

	BIODEGRADABLE?	INFLAMMATION	CELL ATTACHMENT	BIOPRINTING TECHNIQUE[A]	CELL VIABILITY (%)	LIMITATIONS	REFS
GELATIN	Yes	None	Yes	EB, PEI, 2PP	70-99.7%	-	41, 56, 60, 63, 64, 66, 67
HYALURONIC ACID	Yes	-	Yes	EB, PEI	64.4%	Needs to be modified for gelation[97]	98, 99
AGAROSE	Yes	-	Yes	EB	60-90%	-	100, 101, 102, 103
CARRAGEENAN	No	-	-	EB	>80%	Only two of the three family	107, 174

						members form gels[105]	
METHYL CELLULOSE	Yes	-	No	EB, MVB	~80-90%	Can only be used as supporting material[53]	13, 112
COLLAGEN	Yes	None	Yes	MVB, EB, IBP, DOD, LBP	46-99%	-	9, 70, 71, 72, 74, 75, 76, 175
CHITOSAN	Yes	-	-	EB	~75%	-	103
GELLAN GUM	Yes	-	No	EB	60-90%	Only undergoes gelation by addition of cations[77]	34, 129, 176

ELASTIN	Yes	-	Yes	LBP	-	Hard to extract, synthetic counterpart is used[77]	177
SILK FIBROIN	Yes	None	Yes	EB, IBP, MVB	70-96%	Needs H-bond breaking before usage[77]	83, 84, 85, 175, 178, 179
PLURONIC	No	-	Yes	EB, MVB	62-86%	Only for short-term cell viability[53]	14, 113, 115, 116
PEG	Yes	None	No	EB, MVB	75.5-94%	Mostly used as crosslinker	117, 118, 119
PNIPAAM	No	-	-	EB	80-97%	Mostly	31

						combined with HA or alginate for biocompatibility[53]	
ALGINATE	Yes	None	If modified with cell adhesion ligands	EB, LIFT, MVB	77-100%	-	91, 92, 93, 94, 112
FIBRIN	Yes	Minimal	Yes	TIP, IBP, EB, LBP, LIFT, DOD	74-100%	Limited long-term stability	87, 88, 89, 175, 180
DECELLULARIZED ECM	Yes	None	Yes	EB	≥95%	Decellularization can cause loss of mechanical strength[146]	147, 148

[A] EB: extrusion-based; PEI: piezo-electric inkjet; 2PP: two-photon polymerization; MVB: micro-valve bioprinting; IBP: inkjet bioprinting; TIP: thermal inkjet printing; LBP: laser-based printing; DOD: drop-on-demand